JCI The Journal of Clinical Investigation

# The LRF transcription factor regulates mature B cell development and the germinal center response in mice

Nagisa Sakurai, … , Ravi Bhatia, Takahiro Maeda

*J Clin Invest.* 2011;121(7):2583-2598. https://doi.org/10.1172/JCI45682.

**Research Article** **Immunology**

B cells play a central role in immune system function. Deregulation of normal B cell maturation can lead to the development of autoimmune syndromes as well as B cell malignancies. Elucidation of the molecular features of normal B cell development is important for the development of new target therapies for autoimmune diseases and B cell malignancies. Employing B cell–specific conditional knockout mice, we have demonstrated here that the transcription factor leukemia/lymphoma-related factor (LRF) forms an obligate dimer in B cells and regulates mature B cell lineage fate and humoral immune responses via distinctive mechanisms. Moreover, LRF inactivation in transformed B cells attenuated their growth rate. These studies identify what we believe to be a new key factor for mature B cell development and provide a rationale for targeting LRF dimers for the treatment of autoimmune diseases and B cell malignancies.



# The LRF transcription factor regulates mature B cell development and the germinal center response in mice

Nagisa Sakurai,[1] Manami Maeda,[1] Sung-Uk Lee,[1] Yuichi Ishikawa,[1] Min Li,[2] John C. Williams,[3] Lisheng Wang,[1] Leila Su,[3] Mai Suzuki,[1] Toshiki I. Saito,[4] Shigeru Chiba,[5] Stefano Casola,[6] Hideo Yagita,[7] Julie Teruya-Feldstein,[8] Shinobu Tsuzuki,[9] Ravi Bhatia,[1] and Takahiro Maeda[1]

[1]Division of Hematopoietic Stem Cell and Leukemia Research, [2]Department of Information Sciences, and [3]Department of Molecular Medicine, Beckman Research Institute of City of Hope, Duarte, California, USA. [4]Clinical Research Center, National Hospital Organisation Nagoya Medical Center, Nagoya, Japan. [5]Department of Clinical and Experimental Hematology, Graduate School of Comprehensive Human Sciences, University of Tsukuba, Ibaraki, Japan. [6]Istituto FIRC di Oncologia Molecolare, Milan, Italy. [7]Department of Immunology, Juntendo University School of Medicine, Tokyo, Japan. [8]Department of Pathology, Memorial Sloan-Kettering Cancer Center, New York, New York, USA. [9]Division of Molecular Medicine, Aichi Cancer Center Research Institute, Nagoya, Japan.

**B cells play a central role in immune system function. Deregulation of normal B cell maturation can lead to the development of autoimmune syndromes as well as B cell malignancies. Elucidation of the molecular features of normal B cell development is important for the development of new target therapies for autoimmune diseases and B cell malignancies. Employing B cell–specific conditional knockout mice, we have demonstrated here that the transcription factor leukemia/lymphoma-related factor (LRF) forms an obligate dimer in B cells and regulates mature B cell lineage fate and humoral immune responses via distinctive mechanisms. Moreover, LRF inactivation in transformed B cells attenuated their growth rate. These studies identify what we believe to be a new key factor for mature B cell development and provide a rationale for targeting LRF dimers for the treatment of autoimmune diseases and B cell malignancies.**

## Introduction

HSCs give rise to immature B cells in the BM, which subsequently migrate to the secondary lymphoid organs, such as the LNs and spleen. The vast majority of newly formed BM B cells die at the transitional B cell stage during the following few days and fail to enter the long-lived mature B cell pool, which mainly consists of B1, follicular B (FOB), and marginal zone B (MZB) cells in the secondary lymphoid organs. During B cell maturation, signals driven by cell-surface receptors and downstream transcription factors must be regulated in a coordinated fashion to maintain mature B cell homeostasis. In particular, both B cell antigen receptor (BCR) and BAFF, the B cell–activating factor belonging to the TNF family, relay crucial signals for mature B cell development and survival, while the Notch pathway regulates MZB cell development (1–5).

B cells are indispensable for humoral immunity, as they ultimately give rise to antibody-secreting plasma cells. During T cell–dependent (TD) antibody responses, naive B cells form germinal centers (GCs), a distinct histologic structure found in secondary lymphoid organs. Naive B cells become activated upon interaction with T cells and antigen-presenting cells and begin to rapidly proliferate and form the characteristic GC structure, in which 2 major genetic changes occur: somatic hypermutation (SHM) and class switch recombination (CSR). SHM modifies the affinity of the BCR for the cognate antigen by introducing predominantly point mutations into the variable region of Ig genes, while CSR replaces the constant regions of the Ig heavy (IgH) chain with those of other isotypes and allows the expression of antibodies that have the same antigen specificity but are different secondary IgH isotypes. These processes, accompanied by exponential cell proliferation and subsequent apoptosis, must be tightly regulated, as deregulation of GC reactions could lead to malignant transformation and development of autoimmune diseases (6). The protooncogene B cell lymphoma 6 (BCL6), a transcriptional repressor that belongs to the POK (POZ/BTB and Krüppel-type zinc finger) protein family (6), is one of the critical genes for the GC reaction. The BCL6 protein is predominantly expressed in GCB cells, and loss of the *Bcl6* gene in mice impedes GC development (7, 8), while its constitutive activation leads to enhanced GC formation (9), confirming its crucial role in GC reactions.

Leukemia/lymphoma-related factor (LRF) (10), also known as Pokemon (11), Zbtb7a, FBI-1, and OCZF, is a POK transcriptional repressor. LRF acts as a protooncogene by transcriptionally repressing the tumor suppressor alternative reading frame (ARF). Lrf-deficient mouse embryonic fibroblasts (MEFs) show a replicative senescence phenotype due to high p19Arf activity, while Lrf overexpression, in collaboration with an additional oncogene, leads to oncogenic transformation of MEFs (11). Furthermore, Lck-Eμ-Lrf mice, in which Lrf is ectopically expressed in both immature B and T cells, develop fatal lymphoblastic lymphoma, and more importantly, LRF protein was highly expressed in 60%–80% of human non-Hodgkin lymphoma (NHL) cases (11).

LRF also acts as a master regulator of cellular differentiation and lineage fate decision in hematopoietic lineages. In erythroid cells, LRF is necessary for the survival of terminally differentiating erythroblasts (12). Lrf KO mice are embryonic lethal due to anemia, and adult mice ($Lrf^{Flox/Flox}$ Mx1 $Cre^{+}$ mice) with conditional inactivation of the *Lrf* gene also demonstrate a block in terminal erythroid differentiation, leading to erythropoietin-resistant macrocytic anemia. Gata1, a key transcription factor in erythroid development,

**Conflict of interest:** The authors have declared that no conflict of interest exists.
**Citation for this article:** *J Clin Invest.* 2011;121(7):2583–2598. doi:10.1172/JCI45682.

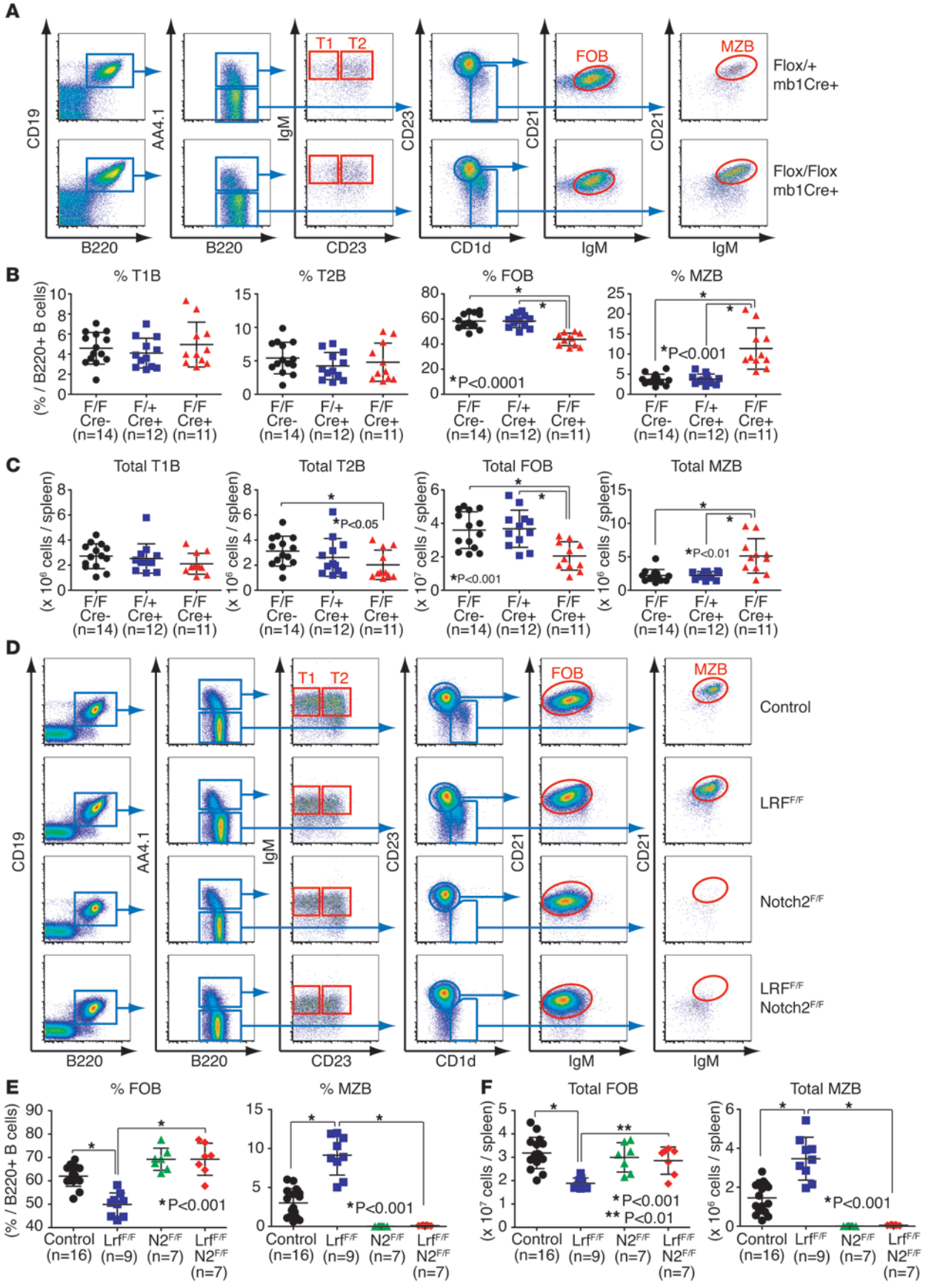
A
CD19
B220
AA4.1
B220
IgM
CD23
T1
T2
CD23
CD1d
CD21
IgM
FOB
CD21
IgM
MZB
Flox/+
mb1Cre+
Flox/Flox
mb1Cre+
B
% T1B
% T2B
% FOB
% MZB
(% / B220+ B cells)
*P<0.0001
*P<0.001
F/F Cre- (n=14)
F/+ Cre+ (n=12)
F/F Cre+ (n=11)
C
Total T1B
Total T2B
Total FOB
Total MZB
(x 10^6 cells / spleen)
(x 10^7 cells / spleen)
*P<0.05
*P<0.001
*P<0.01
D
CD19
B220
AA4.1
B220
IgM
CD23
T1
T2
CD23
CD1d
CD21
IgM
FOB
CD21
IgM
MZB
Control
LRF^F/F
Notch2^F/F
LRF^F/F Notch2^F/F
E
% FOB
% MZB
(% / B220+ B cells)
*P<0.001
*P<0.001
Control (n=16)
Lrf^F/F (n=9)
N2^F/F (n=7)
Lrf^F/F N2^F/F (n=7)
F
Total FOB
Total MZB
(x 10^7 cells / spleen)
(x 10^6 cells / spleen)
*P<0.001
** P<0.01
*P<0.001

**Figure 1**
LRF regulates B cell lineage fate. (**A**) FACS profiles of splenic B cells in control (top) and B cell–specific Lrf KO mice (bottom). Dot graphs demonstrate proportions (**B**) and absolute counts (**C**) of FOB and MZB cells within the splenic mononuclear cells. Cre-negative control (Flox/Flox; *n* = 7), Lrf heterozygous (Flox/+ Cre$^+$; *n* = 12), and B cell–specific Lrf KO mice (Flox/Flox Cre$^+$; *n* = 11) were analyzed. Horizontal black bars show average value; error bars represent SD. (**D**) Representative FACS profiles of mature B cell compartments in control (mb-1 Cre-), Notch2 single (Notch2$^{Flox/Flox}$ mb-1 Cre$^+$), Lrf single (LRF$^{Flox/Flox}$ mb-1 Cre$^+$), and Lrf/Notch2 double-KO (Lrf$^{Flox/Flox}$Notch2$^{Flox/Flox}$ mb-1 Cre$^+$) mice. Dot graphs demonstrate proportions (**E**) and absolute counts (**F**) of mature B cell compartments in each genotype. Horizontal black bars indicate average value; error bars indicate SD.

transcriptionally activates Lrf, and Lrf, in turn, represses the pro-apoptotic factor Bim in an p19Arf/p53-independent fashion (12). Genetic loss of the *Bim* gene partially rescues the embryonic lethality and anemia phenotype seen in Lrf KO mice (12).

During the early lymphoid lineage specification stage, LRF critically regulates the T versus B lymphoid lineage fate decision in the BM at the HSC/progenitor levels. Inducible inactivation of the *Lrf* gene in mouse HSCs results in extrathymic double-positive T cell development in the BM at the expense of B cell development (13). Aberrant lineage specification was caused by Notch-dependent mechanisms, as γ secretase inhibitor, a potent Notch inhibitor, treatment rescued normal lymphoid development in Lrf$^{Flox/Flox}$ Mx1 Cre$^+$ mice (13). Although these data clearly indicate that Lrf is necessary for normal lymphoid lineage fate determination via repressing Notch, the precise mechanisms by which LRF interferes with the Notch signal remain elusive.

Notch is necessary for the emergence of definitive hematopoiesis in embryos (14) and is a master regulator for lymphoid lineage fate determination (15). In particular, Notch is essential for T cell differentiation from HSCs/progenitors, as mutant mouse models lacking Notch components demonstrate lack of T cells and concomitant development of immature B cells in the thymus (16–18). Conversely, constitutive activation of the Notch pathway at HSC/progenitor stages leads to aberrant T cell development and eventually causes leukemic transformation (19). Furthermore, activating NOTCH1 point mutations have been found at high frequency in T lymphoblastic leukemia cases (20). Notch also plays a role in mature B cell lineage fate decisions. Inactivation of components of the Notch pathways in B cells in mice (Notch2, Rbpjκ, Maml1, Delta-like 1, Mib1, fringes, and Adam10) impedes MZB cell development in the spleen, with a concomitant increase in FOB cells (1–4, 21–23). Conversely, deletion of the *Mint/Sharp* gene, a suppressor of Notch signaling, leads to an increase in MZB cells and reduction in FOB cells (5).

Although previous studies underscore the roles for LRF in lymphoid lineage commitment and oncogenesis, it is unclear whether LRF is necessary for the development and maintenance of "committed" B cells, particularly GCB cells, in which the LRF protein is highly expressed. Here we show, using genetic and biochemical approaches, that LRF plays critical roles in mature B cell development and function via distinct mechanisms.

## Results

*Lrf is dispensable for the maintenance of BM B cells*. We established B cell–specific Lrf conditional KO mice (Lrf$^{Flox/Flox}$ mb-1 Cre$^+$), in which Cre expression was restricted to B cells after the pro–B cell stage (24). Analysis of BM B cell populations of Lrf$^{Flox/Flox}$ mb-1 Cre$^+$ mice showed that B cell compartments in the BM were grossly normal in the absence of the *Lrf* gene. Proportions of pre-pro–B (Lin$^-$B220$^+$IgM$^-$CD43$^+$CD19$^-$), pro–B (Lin$^-$B220$^+$IgM$^-$CD43$^+$CD19$^+$), pre–B (Lin$^-$B220$^+$IgM$^-$CD43$^-$CD19$^+$), and immature B (Lin$^-$B220$^+$IgM$^+$CD43$^-$CD19$^+$) cells in the BM were comparable to those of controls (Supplemental Figure 1, A and B; supplemental material available online with this article; doi:10.1172/JCI45682DS1). Quantitative real-time PCR confirmed the *Lrf* gene was efficiently deleted in BM-CD19$^+$ B cells (Supplemental Figure 1C), and no Lrf protein was detected (Supplemental Figure 1D), confirming the conditional inactivation of the *Lrf* gene in B cells. Therefore, despite its critical role in lymphoid lineage fate determination at the HSC/progenitor stages (13), Lrf was dispensable for maintenance of BM B cells. These findings were consistent with the fact that treatment with γ secretase inhibitor restored normal B cell development in Lrf$^{Flox/Flox}$ Mx1 Cre$^+$ mice (13).

*Lrf regulates mature B cell lineage fate*. We next characterized mature B cell development in secondary lymphoid organs of Lrf$^{Flox/Flox}$ mb-1 Cre$^+$ mice. Proportions of FOB cells (B220$^+$CD19$^+$AA4.1$^-$CD1d$^-$CD23$^+$IgM$^{lo/-}$CD21$^{lo}$) were decreased, and those of MZB cells (B220$^+$CD19$^+$AA4.1$^-$CD1d$^+$CD23$^-$IgM$^{hi}$CD21$^{hi}$) were significantly increased in the spleens of Lrf$^{Flox/Flox}$ mb-1 Cre$^+$ mice, while transitional B cells (T1B and T2B) were largely unaffected (Figure 1, A and B). Furthermore, absolute numbers of FOB cells were lower and those of MZB cells greater in Lrf$^{Flox/Flox}$ mb-1 Cre$^+$ mice (Figure 1C), indicating that FOB versus MZB lineage fate determination is unbalanced in the absence of the *Lrf* gene.

Considering that (a) Lrf opposes Notch function at the HSC/progenitor levels (13) and (b) hairy and enhancer of split 1 (*Hes1*), a Notch target gene, was upregulated in Lrf-deficient transitional B cells (Supplemental Figure 2A), we hypothesized that the aberrant MZB versus FOB lineage fate decision in Lrf$^{Flox/Flox}$ mb-1 Cre$^+$ mice accounted for the high Notch activity in Lrf-deficient cells. To test this, Notch2/Lrf double-conditional KO mice (Lrf$^{Flox/Flox}$Notch2$^{Flox/Flox}$mb-1 Cre$^+$) were generated, and their mature B cell development analyzed. Loss of Notch2 not only reduced MZB cell differentiation, but also enhanced FOB cell development in Lrf$^{Flox/Flox}$ mb-1 Cre$^+$ mice (Figure 1, D and E). Furthermore, the absolute numbers of Lrf-deficient FOB cells recovered to control levels (Figure 1F).

There are 5 Notch ligands in mammals (Jagged-1,-2, Delta-like-1, -3, and -4), and, among them, Delta-like-1 (Dll1) is highly expressed in the splenic MZ (22). Conditional inactivation of the *Dll1* gene led to a reduction of MZB cells and concomitant increase of FOB cells (1), indicating that Dll1/Notch2 interaction plays a major role in FOB versus MZB lineage fate determination. To determine whether the Dll1/Notch2 interaction is a prerequisite for Notch2 activation in Lrf-deficient B cells, Lrf$^{Flox/Flox}$ mb-1 Cre$^+$ mice were treated with anti-Dll1 antibody (Supplemental Figure 2B). Proportions of MZB cells were equivalent to the levels of control after Dll1 treatment (Supplemental Figure 2, C and D), suggesting the active Notch phenotype seen in Lrf$^{Flox/Flox}$ mb-1 Cre$^+$ mice was caused in a ligand-dependent rather than ligand-independent fashion.

*Lrf is required for GC formation*. We previously found that the LRF protein was highly expressed in normal GC and diffuse large B cell lymphoma (DLBCL) tissues (11). To determine the magnitude of Lrf loss in the GC response in vivo, we characterized secondary lymphoid organs of Lrf$^{Flox/Flox}$ mb-1 Cre$^+$ mice after TD antigen stimulation. Eight- to ten-week-old mice were immunized with 4-hydroxy-3-nitro-

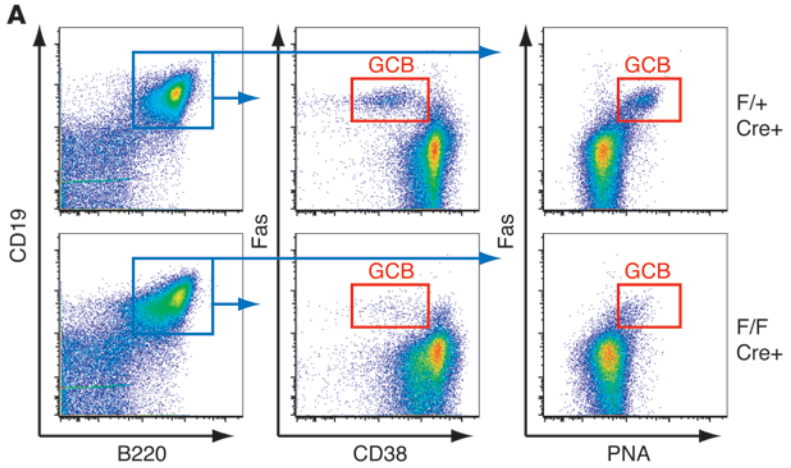
A
CD19
Fas
B220
GCB
CD38
Fas
PNA
F/+
Cre+
F/F
Cre+

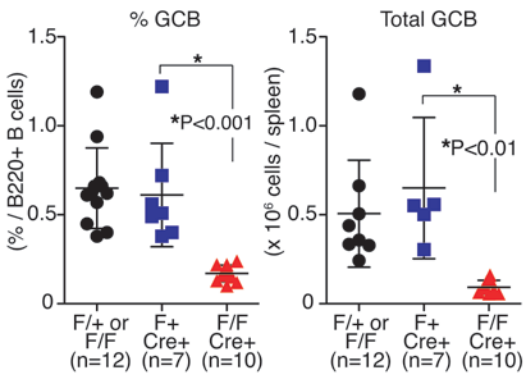
B
% GCB
Total GCB
(% / B220+ B cells)
(x 10⁶ cells / spleen)
*P<0.001
*P<0.01
F/+ or F/F (n=12)
F+ Cre+ (n=7)
F/F Cre+ (n=10)

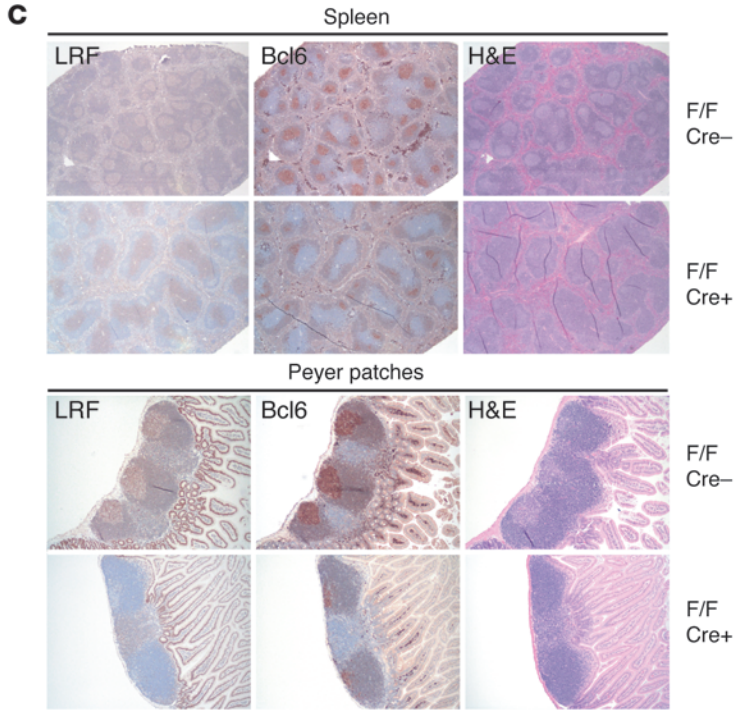
C
Spleen
LRF
Bcl6
H&E
F/F Cre–
F/F Cre+
Peyer patches

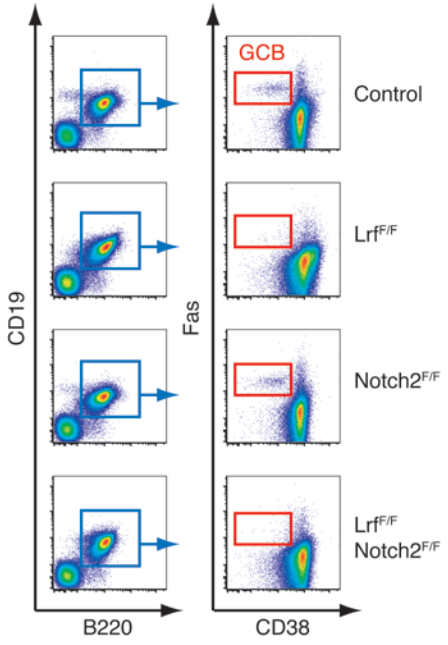
D
CD19
Fas
B220
GCB
CD38
Control
Lrf F/F
Notch2 F/F
Lrf F/F Notch2 F/F

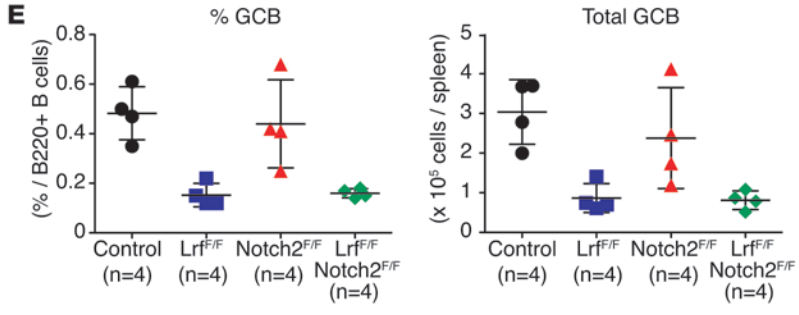
E
% GCB
Total GCB
(% / B220+ B cells)
(x 10⁵ cells / spleen)
Control (n=4)
Lrf F/F (n=4)
Notch2 F/F (n=4)
Lrf F/F Notch2 F/F (n=4)

**Figure 2**
LRF is necessary for GC formation. (**A**) FACS profiles of splenic GC cells. Control ($Lrf^{Flox/+}$ mb-1 $Cre^+$) and KO ($Lrf^{Flox/Flox}$ mb-1 $Cre^+$) mice were intraperitoneally injected with NP-CGG. Splenocytes were harvested 2 weeks after immunization and analyzed with multi-color FACS using the indicated cell surface markers. (**B**) There were significantly fewer GC cells in $Lrf^{Flox/Flox}$ mb-1 $Cre^+$ mice. Dot graphs demonstrate proportions (left) and absolute numbers (right) of GC cells ($DAPI^-B220^+CD19^+CD38^-FAS^+$) of each genotype. Cre-negative control ($n = 12$), Lrf heterozygous (Flox/+ $Cre^+$; $n = 7$), and B cell–specific Lrf KO (Flox/Flox $Cre^+$; $n = 10$) mice were analyzed. Horizontal black bars indicate average value; error bars indicate SD. (**C**) IHC analysis of secondary lymphoid organs. GC formation in Peyer patches (bottom) and spleens (top) was examined by IHC. GCs are recognized as clusters of Bcl6-positive cells. Original magnification, ×40 (spleen); ×100 (Peyer patches). (**D**) FACS profiles of splenic GCB cells for control, Lrf KO ($Lrf^{Flox/Flox}$ mb-1 $Cre^+$), Notch2 KO ($Notch2^{Flox/Flox}$ mb-1 $Cre^+$), and Lrf/Notch2 double-KO ($Lrf^{Flox/Flox}Notch2^{Flox/Flox}$ mb-1 $Cre^+$) mice. The reduction in GCB cells was not recovered by loss of the *Notch2* gene. (**E**) Frequencies and absolute numbers of GCB cells for each genotype. Horizontal black bars indicate average value; error bars indicate SD.

phenylacetyl hapten-coupled chicken gamma globulin (NP-CGG), and their spleens and Peyer patches were analyzed 2 weeks after immunization. Although a robust GC reaction was induced in control mice upon immunization, only a few GC cells ($B220^+CD19^+FAS^+CD38^{dim}PNA^+$) were observed in spleens of $Lrf^{Flox/Flox}$ mb-1 $Cre^+$ mice (Figure 2A). Proportions and absolute numbers of GCB cells were significantly less in $Lrf^{Flox/Flox}$ mb-1 $Cre^+$ mice (Figure 2B). The reduction in GCB cells was also confirmed via immunohistochemical analysis, as GCs, which were identified as clusters of Bcl6-positive cells, were markedly reduced in size in the spleen and Peyer patches of $Lrf^{Flox/Flox}$ mb-1 $Cre^+$ mice (Figure 2C). Of note, the defect in GC formation was not rescued by Notch2 loss, as the perturbed GC formation was seen in Lrf/Notch2 double-KO mice (Figure 2, D and E).

*TD antigen response is impaired in $Lrf^{Flox/Flox}$ mb-1 $Cre^+$ mice*. The GC reaction is essential for creating high-affinity antibodies against a variety of antigens, and both SHM and CSR, which are mediated by activation-induced cytidine deaminase (AID), play central roles during the process. To determine whether loss of Lrf in B cells leads to defects in CSR in vivo, we measured the titers of class-switched Ig in the serum of $Lrf^{Flox/Flox}$ mb-1 $Cre^+$ mice. Baseline serum titers of class-switched antibodies ($IgG_1$, $IgG_{2b}$, and $IgG_3$) were perturbed in $Lrf^{Flox/Flox}$ mb-1 $Cre^+$ mice (Figure 3A). We further examined the primary, secondary, and tertiary antibody responses of mutant mice against the TD antigen NP-CGG. Mice were immunized with alum-precipitated NP-CGG and serum samples collected every 14 days for 8 weeks, after which mice were boosted, and serum titers for NP-specific IgG1 antibody measured. Responses to NP-specific antigen were severely impaired in $Lrf^{Flox/Flox}$ mb-1 $Cre^+$ mice (Figure 3B), which also had significantly fewer BM long-lived plasma cells (Figure 3C). In contrast, anti-NP responses to NP-Ficoll, a type 2 T cell–independent (TID) antigen, were not perturbed. NP-specific IgM responses of $Lrf^{Flox/Flox}$ mb-1 $Cre^+$ mice were equivalent to those of controls at days 7 and 14 after immunization (Figure 3D). The capacity of Lrf-deficient B cells to undergo CSR was unaffected in vitro (Supplemental Figure 3A), while Lrf-deficient B cells proliferated to a lesser extent than control upon LPS stimulus (Supplemental Figure 3B). Thus, the impaired CSR seen in $Lrf^{Flox/Flox}$ mb-1 $Cre^+$ mice was likely due to lack of absolute GCB cell numbers rather than defective Aid function.

To investigate whether LRF is required for SHM, frequencies of somatic mutations in the rearranged V186.2 genes, which are used by B cells of C57BL/6 mice in response to the hapten NP, were examined. GCB cells from control ($Lrf^{Flox/+}$ mb-1 $Cre^+$) and Lrf-KO mice ($Lrf^{Flox/Flox}$ mb-1 $Cre^+$) were FACS sorted 14 days after NP-CGG immunization and the degree of SHM in rearranged V186.2 genes analyzed. Frequencies and overall patterns of SHM were not substantially perturbed in Lrf-deficient GCB cells (Supplemental Figure 3, C and D).

Because the *Lrf* gene is deleted in naive B cells before they are challenged by TD antigen in $Lrf^{Flox/Flox}$ mb-1 $Cre^+$ mice, it is still possible that Lrf is required for commitment to rather than maintenance of GCB cells. To distinguish these possibilities, we used C-gamma-1 Cre transgenic mice (Cγ1 Cre), in which Cre recombinase is induced by transcription of the Ig gamma-1 constant region gene segment (Figure 3E and ref. 25). Lrf inactivation in GCB cells ($Lrf^{Flox/Flox}$ Cγ1 $Cre^+$) led to reduction of GCB cell numbers (Figure 3F). Furthermore, primary and secondary antibody responses to TD antigen were impaired in $Lrf^{Flox/Flox}$ Cγ1 $Cre^+$ mice. Serum titers of NP-specific IgG1b antibody were significantly perturbed in $Lrf^{Flox/Flox}$ Cγ1 $Cre^+$ mice (Figure 3G). We measured the titers of the IgG1b allotype, as the Cγ1 Cre cassette was inserted into an IgH locus of an allotype affecting IgG1a expression (25). These data indicate that Lrf is required for the maintenance and function of GCB cells rather than commitment to GCB cells.

*Lrf is indispensable for GCB cell proliferation and survival*. Because the LRF deletion was limited to B cells and overall GC architectures, albeit small, (Figure 2C), remained intact in $Lrf^{Flox/Flox}$ mb-1 $Cre^+$ mice, inefficient GC formation was likely due to (a) intrinsic defects in GCB cell proliferation and/or (b) increased GCB cell apoptosis. To elucidate the overall effect of Lrf loss in the GCB cell transcriptome, gene expression microarray analysis of FACS-sorted GCB cells was performed. $Lrf^{Flox/+}$ mb-1 $Cre^+$ mice were used as a control to normalize the potential effects of Cre recombinase, and 4 RNA samples for each genotype were used for the analysis. Lrf-deficient GCB cells demonstrated a unique gene expression signature, as an unsupervised hierarchical clustering analysis precisely predicted the genotype of each sample (Supplemental Figure 4A). A total of 1,518 probe sets were up- or downregulated more than 1.5-fold in Lrf-deficient GCB cells, and functional annotation clustering was performed using a DAVID program (26). Statistically significant and overrepresented biological annotations are listed in Table 1. Annotations representing cellular proliferation (e.g., ribosome, metabolic process, mitochondria) were significantly enriched in gene sets that were downregulated in Lrf-deficient GCB cells. Gene Set Enrichment Analysis (GSEA) also showed that Lrf-deficient GCB cells were defective in growth-promoting signaling pathways and ribosomal biogenesis (Figure 4B), suggesting proliferative defects in the absence of the *Lrf* gene.

To assess cell-cycle status and proliferation rates of Lrf-deficient GCB cells, short-term kinetic analysis of 5-ethynyl-2′-deoxyuridine (EdU) incorporation was performed. Mice were intraperitoneally injected with EdU 5 hours before analysis, and splenic GCB cells were analyzed for the degree of EdU incorporation in combination with surface marker and DAPI DNA staining on day 7 after NP-CGG immunization. As expected, EdU was efficiently incorporated into control GCB cells (Figure 4C). However, EdU incorporation was significantly impaired in Lrf-deficient GCB cells, and the frequencies of GCB cells in S phase were lower in $Lrf^{Flox/Flox}$ mb-1 $Cre^+$ mice (Figure 4D). GCB cells can be detected by FACS as early as 4 days after immuniza-

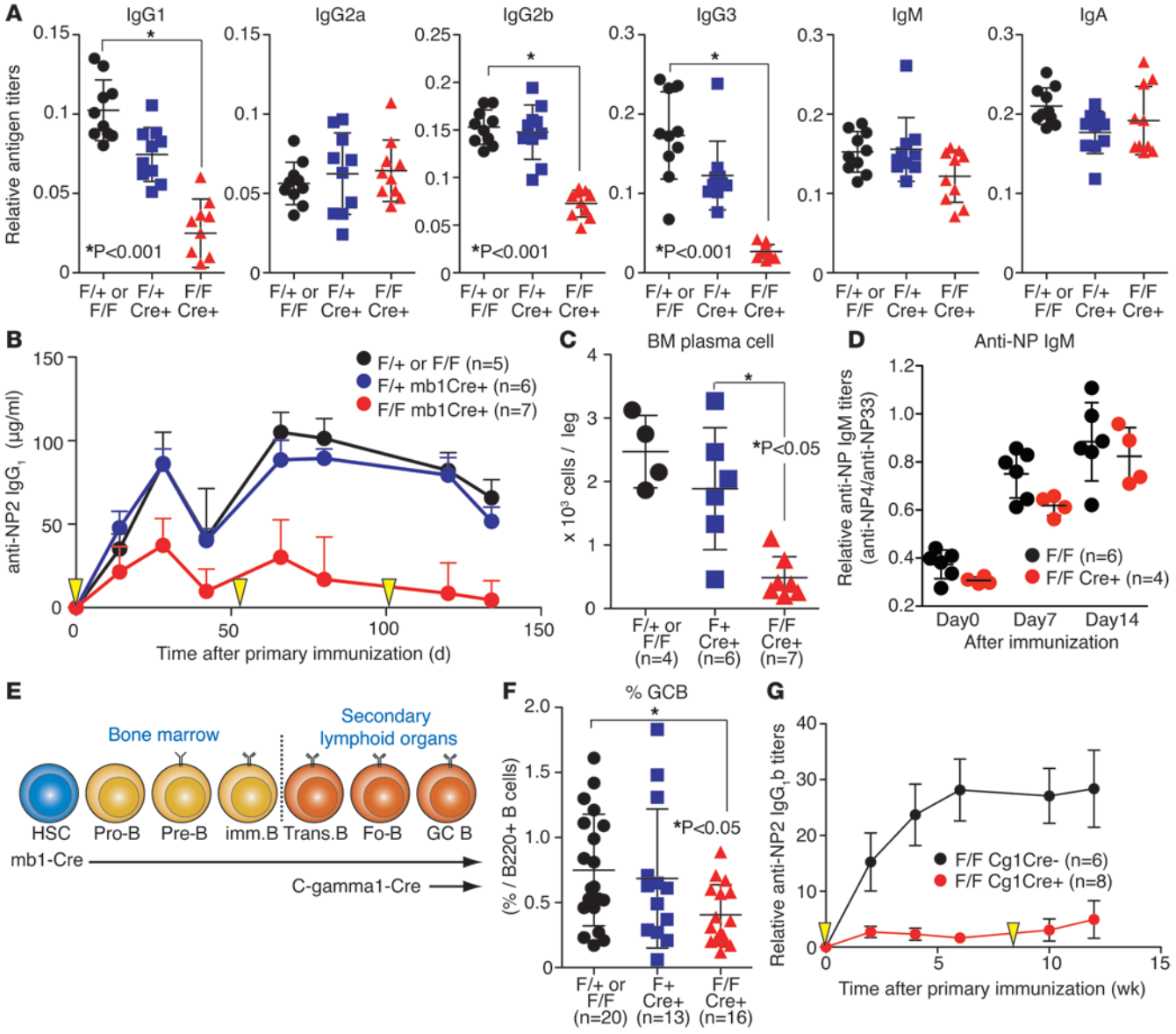


**Figure 3**

Impaired TD antigen response in Lrf$^{Flox/Flox}$ mb-1 Cre$^{+}$ mice. (**A**) Baseline serum Ig levels as measured by ELISA ($n$ = 10, for each genotype). Horizontal black bars indicate average value; error bars indicate SD. (**B**) Primary, secondary, and tertiary responses against TD antigen in Lrf$^{Flox/Flox}$ mb-1 Cre$^{+}$ mice. $y$ axis shows NP-specific IgG1 antibody titers; $x$ axis shows days after primary immunization; yellow arrowheads indicate NP-CGG injections. (**C**) Long-lived plasma cells in the BM were analyzed 154 days after primary immunization. Absolute numbers of BM long-lived plasma cells (B220$^{-}$CD138$^{+}$) are shown. Horizontal black bars indicate average value; error bars indicate SD. (**D**) Humoral response to NP-Ficoll, a TID antigen. Mice were immunized with NP-Ficoll and blood samples collected on the dates indicated. No statistical difference was found in $NP_4/NP_{33}$ binding ratio (indicates presence of high-affinity antibodies). (**E**) Diagram showing that Cre recombinase is specifically activated at the GCB stage in C$\gamma$1 Cre$^{+}$ mice, while Cre is expressed at the pro–B stage in mb1 Cre knockin mice. (**F**) Dot graphs demonstrate proportions of GCB cells of each genotype. Cre-negative control ($n$ = 20), Lrf heterozygous ($n$ = 13), and GCB cell–specific Lrf KO ($n$ = 16) mice were analyzed. (**G**) Primary and secondary responses against TD antigen in Lrf$^{Flox/Flox}$ C$\gamma$1 Cre$^{+}$ mice. $y$ axis shows NP-specific IgG1b antibody titers; $x$ axis shows after primary immunization with NP-CGG; yellow arrows show NP-CGG injections. Horizontal black bars indicate average value; error bars indicate SD.

tion, followed by an exponential increase in cell numbers that peaks on days 7–8 and gradually diminishes 2 weeks after immunization (27). In agreement with the EdU incorporation assay data, the difference in cell numbers between control and Lrf-deficient mice was more evident over time after immunization (Figure 4E).

Two main compartments within the GC, the dark zone (DZ) and light zone (LZ), have been described on the basis of their histological appearance. The DZ is closely packed with lymphocytes, while the LZ contains FO dendritic cells and lymphocytes. Cxcr4, a chemokine receptor, is required for GCB cell positioning in the DZ, and Cxcr4-expressing cells are more abundant in the DZ than in the LZ (28). GCB cells that expressed Cxcr4 at high levels (Cxcr4$^{hi}$) are more active in the cell cycle than Cxcr4$^{lo}$ GCB cells (28); therefore, we investigated what proportion of GCB cells

**Table 1**
Overrepresented biological annotations of genes downregulated in LRF-deficient GCBs

| Annotation cluster | ES[A] | *P* value[B] | GO[C] |
|---|---|---|---|
| Cell migration | 3.37 | 4.31E-04 | 0016477 |
| | | | 0051674 |
| | | | 0006328 |
| Membrane | 3.04 | 9.07E-04 | 0044425 |
| | | | 0016021 |
| | | | 0031224 |
| Ribosome | 11.84 | 1.45E-12 | 0005840 |
| | | | 0003735 |
| | | | 0005198 |
| Cellular metabolic process | 8.9 | 1.27E-09 | 0008152 |
| | | | 0044237 |
| | | | 0044238 |
| Protein metabolic process | 6.36 | 4.35E-07 | 0019538 |
| | | | 0044267 |
| | | | 0044260 |
| Mitochondria | 5.58 | 2.61E-06 | 0005740 |
| | | | 0044429 |
| | | | 0031967 |
| | | | 0031975 |
| | | | 0031966 |
| | | | 0005743 |
| | | | 0019866 |
| RNA splicing | 4.96 | 1.10E-05 | 0008380 |
| | | | 0016071 |
| | | | 0006397 |
| | | | 0005681 |
| Protein localization/transport | 3.88 | 1.32E-04 | 0033036 |
| | | | 0008104 |
| | | | 0045184 |
| | | | 0015031 |
| Ubiqutin ligase | 3.25 | 5.59E-04 | 0008639 |
| | | | 0004842 |
| | | | 0016881 |
| | | | 0019787 |
| | | | 0016879 |

[A]Gene sets were uploaded to the DAVID online analysis tool, and overrepresented annotation clusters demonstrating enrichment score (ES) > 3 are shown. [B]Geometric means of member's modified Fisher exact *P* values in a corresponding annotation cluster. [C]Enriched GO (Gene Ontology) terms within the cluster are also shown.

(Cxcr4$^{hi}$ or Cxcr4$^{lo}$) was mainly affected in the absence of Lrf. As expected, there were considerably fewer highly proliferative Cxcr4$^{hi}$ GCB cells in Lrf$^{Flox/Flox}$ mb-1 Cre$^{+}$ mice (Figure 4F).

We next examined GCB cell apoptosis in the absence of Lrf by measuring the amounts of the active form of caspase-3 and cleaved form of Poly (ADP-ribose) polymerase (PARP), which is a target of the caspase protease activity associated with apoptosis. Mice were immunized with sheep red blood cells (SRBCs), and apoptotic GCB cells were detected by FACS 7 days after immunization. As reported previously, GCB cells (B220$^{+}$CD19$^{+}$CD38$^{dim+}$Fas$^{+}$) underwent apoptosis at a higher rate than non-GCB cells (B220$^{+}$CD19$^{+}$CD38$^{hi+}$Fas$^{-}$) (Figure 4G). Although no histological evidence of excessive apoptosis (e.g., "tingible bodies" inside macrophages) was observed in Lrf-deficient GCs (not shown), caspase activity was significantly greater in Lrf$^{Flox/Flox}$ mb-1 Cre$^{+}$ mice (Figure 4G), indicating that Lrf-deficient GCB cells undergo apoptosis more frequently as compared with controls.

*p19Arf is upregulated in Lrf-deficient GCB cells.* The molecular mechanisms that regulate the balance between exponential proliferation and concomitant apoptosis of GCB cells are not fully understood (6). Since Lrf regulates the p53 pathway by repressing the tumor suppressor p19Arf in MEFs (11), we hypothesized that Lrf could also regulate the p53 pathway via p19Arf repression in the context of GCB cells. In support of this, microarray analysis demonstrated upregulated transcript levels of the *Cdkn2a* gene, consisting of the *p19Arf* and *p16Ink4a* genes, and the *Cdkn1a* gene, a downstream target of the Arf/p53 pathway (not shown). To validate this finding, mRNA levels of p19Arf, p53 and p21 in Lrf-deficient GCB cells were measured by quantitative RT-PCR (qRT-PCR). p19Arf and p21 mRNAs were significantly upregulated in Lrf-deficient GCB cells, while p53 mRNA levels remained unchanged (Figure 5A). Of note, mRNA levels of p16Ink4a, which also resides at the Cdkn2A locus, were undetectable irrespective of genotype, indicating that Lrf loss specifically affects p19Arf expression without affecting the *p16ink4a* gene, as observed in *Lrf*$^{-/-}$ MEFs (not shown) (11). Western blot analysis of FACS-sorted GCB cells showed high p19Arf protein levels in Lrf-deficient GCB cells, whereas no p19Arf protein was detected in control GCB samples (Figure 5B). Immunofluorescence analysis further demonstrated accumulation of nucleolar p19Arf protein in Lrf-deficient GCB cells (Figure 5C). p19Arf upregulation in Lrf-deficient GCB cells was likely due to direct transcriptional derepression of the *p19Arf* gene. Anti-LRF antibody specifically precipitated p19Arf promoter sequences from extracts prepared from primary GCB cells, as revealed by chromatin immunoprecipitation assay (Supplemental Figure 4B).

*Lrf knockdown is toxic to B cell lymphoma cell lines.* Since LRF is highly expressed in DLBCL tissues (11) and necessary for normal GCB cell proliferation and survival (Figures 3 and 4), we next examined LRF protein expression levels in a series of human B cell lymphoma cell lines by Western blot. LRF was highly expressed in all lymphoma cell lines examined, regardless of lymphoma subtype (Figure 6A). To determine whether LRF inactivation affected proliferation of B cell lymphoma cell lines, lentivirus-based inducible shRNA for LRF, which allowed the fate of shRNA-expressing cells to be traced by GFP, was generated (Figure 6B and ref. 29). In this system, shRNA expression is induced upon doxycycline (Dox) treatment (29) and the fate of shRNA-expressing cells can be followed by analyzing the proportions of GFP-positive (shRNA$^{+}$) and -negative (shRNA$^{-}$) cells by FACS over time. We tested 5 different shRNA clones against LRF, and 2 clones that demonstrated efficient LRF knockdown (clones nos. 2 and 4) were subcloned into the inducible lentiviral vector and used for the study (Supplemental Figure 5, A and B). We tested 3 NHL cell lines: OCI–Ly-1 (GCB-like DLBCL), OCI–Ly-3 (activated B cell-like DLBCL), and Ramos (Burkitt lymphoma). Cells that expressed shRNA-LRF, but not cells transduced with empty vector or unrelated shRNA (shRNA-GATA1), demonstrated a proliferative disadvantage as compared with nontransduced (GFP$^{-}$) cells (Figure 6C), indicating a toxic effect of shRNA-LRF in a subset of B cell lymphoma cell lines. The effect of LRF knockdown was likely blunted at later time points, as significant amounts of LRF protein were observed, even in the shRNA-LRF–transduced, GFP-positive cells 17 days after Dox treatment (Supplemental Figure 5, C and D).

LRF-deficient mouse GCB cells led to upregulation of p19ARF and p21, a downstream target of the ARF/p53 pathway (Figure 5A). To examine whether the toxic effects of LRF-shRNAs in lymphoma cell lines were rescued by p21 downregulation,

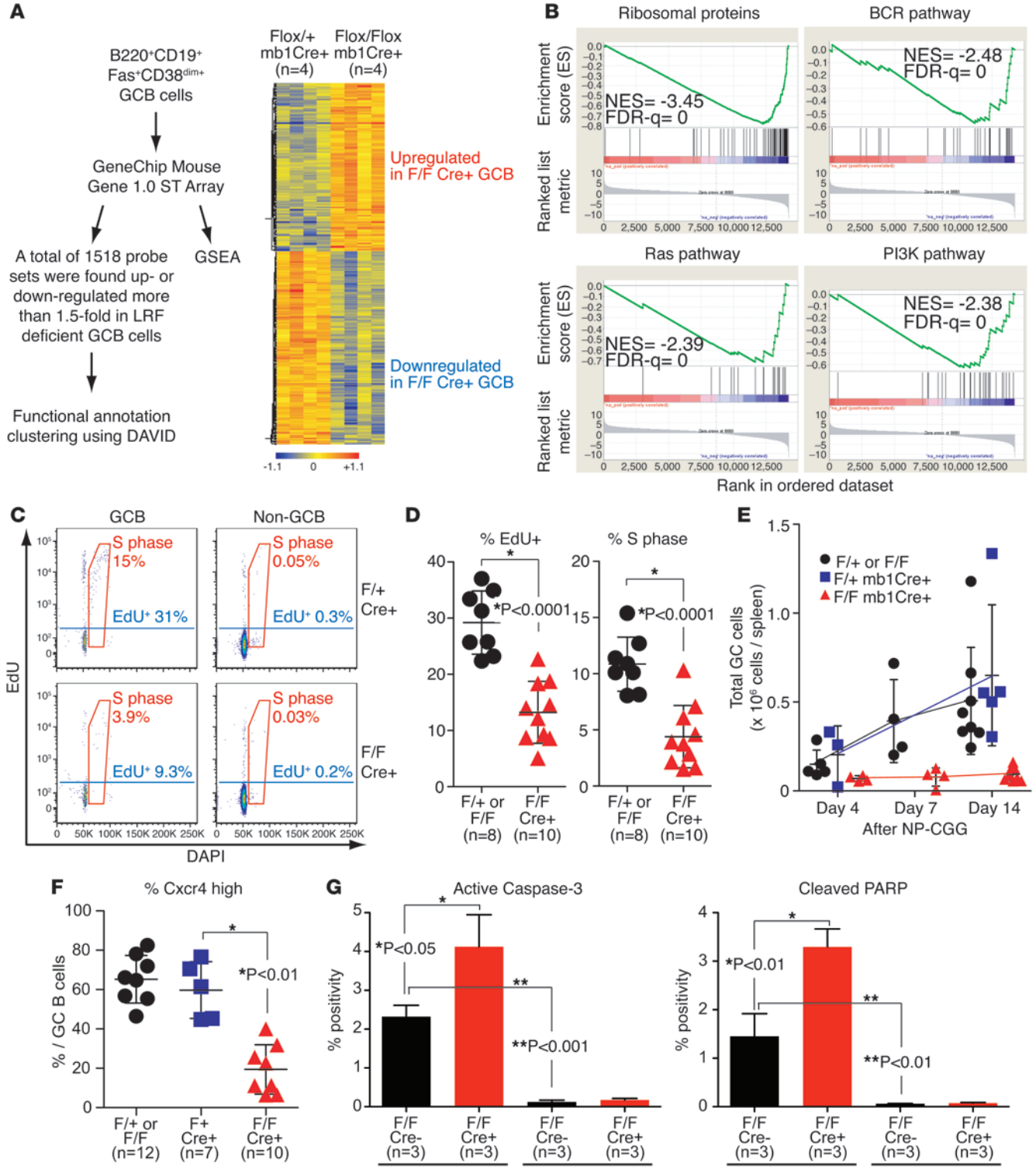
A
B220+CD19+
Fas+CD38dim+
GCB cells
GeneChip Mouse
Gene 1.0 ST Array
A total of 1518 probe sets were found up- or down-regulated more than 1.5-fold in LRF deficient GCB cells
GSEA
Functional annotation clustering using DAVID
Flox/+ mb1Cre+ (n=4)
Flox/Flox mb1Cre+ (n=4)
Upregulated in F/F Cre+ GCB
Downregulated in F/F Cre+ GCB
-1.1
0
+1.1
B
Ribosomal proteins
NES= -3.45
FDR-q= 0
BCR pathway
NES= -2.48
FDR-q= 0
Ras pathway
NES= -2.39
FDR-q= 0
PI3K pathway
NES= -2.38
FDR-q= 0
Enrichment score (ES)
Ranked list metric
Rank in ordered dataset
C
GCB
Non-GCB
S phase 15%
EdU+ 31%
S phase 0.05%
EdU+ 0.3%
S phase 3.9%
EdU+ 9.3%
S phase 0.03%
EdU+ 0.2%
F/+ Cre+
F/F Cre+
EdU
DAPI
D
% EdU+
*P<0.0001
% S phase
*P<0.0001
F/+ or F/F (n=8)
F/F Cre+ (n=10)
E
F/+ or F/F
F/+ mb1Cre+
F/F mb1Cre+
Total GC cells (x 10^6 cells / spleen)
Day 4
Day 7
Day 14
After NP-CGG
F
% Cxcr4 high
% / GC B cells
*P<0.01
F/+ or F/F (n=12)
F+ Cre+ (n=7)
F/F Cre+ (n=10)
G
Active Caspase-3
*P<0.05
**P<0.001
% positivity
F/F Cre- (n=3)
F/F Cre+ (n=3)
GCB
Non-GCB
Cleaved PARP
*P<0.01
**P<0.01

**Figure 4**
Lrf is required for GCB cell proliferation and survival. (**A**) GCB cells were isolated from spleens of $Lrf^{Flox/+}$ mb-1 $Cre^+$ and $Lrf^{Flox/Flox}$ mb-1 $Cre^+$ mice and gene expression microarray analysis performed. A total of 706 probes were downregulated and 812 probes were upregulated more than 1.5-fold in LRF-deficient GCB cells. (**B**) Representative results of GSEA analysis. NES, normalized enrichment score; FDR-q, false discovery rate *q* value. (**C**) Mice were immunized with NP-CGG. On day 7 after immunization, EdU was intraperitoneally injected 5 hours before analysis. FACS analysis of EdU incorporation in GCB cells ($B220^+CD19^+CD38^-FAS^+$) and non-GCB cells ($B220^+CD19^+CD38^+FAS^-$). (**D**) Graphs show proportions of EdU-positive (left) and S phase (right) cells in GC–B cells. (**E**) Time-course analysis of absolute GCB cell numbers. *x* axis shows days after NP-CGG immunization. (**F**) Dot graph demonstrates the proportion of $Cxcr4^{hi}$ cells within GCB cells. (**G**) Mice were immunized with SRBCs, and apoptosis of GCB cells was measured by active caspase-3 staining (left) and cleaved PARP staining (right) 7 days after immunization. Horizontal black bars indicate average value; error bars indicate SD.

LRF was inducibly knocked down via shRNA in the presence or absence of shRNA against p21 and the proportions of GFP-positive (shRNA-$LRF^+$) cells were followed by FACS over time. Two different p21 shRNA clones were used, both of which demonstrated efficient knockdown of the p21 transcript upon Dox treatment (Supplemental Figure 5E). Proliferation of shRNA-LRF–expressing cells was partially restored only in Ramos cells (Figure 6D), suggesting the toxic effects of shRNA-LRF in Ly-1 and Ly-3 cells might be attributed to p21-independent mechanisms. It is worth noting that p21 response to doxorubicin treatment is more evident in Ramos cells (Supplemental Figure 5E) and only Ramos cells showed a proliferative advantage upon p21 knockdown among the 3 cell lines (not shown).

*LRF forms a dimer in B cells*. Our data indicate that LRF is necessary for the proliferation and survival of normal and malignant GCB cells, suggesting that LRF could be a therapeutic target for B cell malignancies and autoimmune diseases. POK proteins normally exist as dimers or oligomers that interact through the POZ domain, and dimer formation is critical for their cellular localization, DNA-binding capacity, and transcriptional activity (30, 31). To investigate whether LRF forms dimers or large protein complexes in cells, we performed a continuous sucrose gradient analysis on LRF in protein extracts from Ly-1 cells, a GC-type DLBCL cell line. LRF protein sedimented to a region in the gradient similar to that of BCL6 (Figure 7A). Moreover, LRF protein (60 kDa) was not detected in the region where E2A monomers (65 kDa) reside, suggesting that LRF protein does not exist as a monomer and forms an obligate dimer or high molecular weight protein complex in cells.

Given the potential significance of dimerization for LRF function, we next asked which amino acid residues were required for LRF-POZ dimerization. We first performed computational analysis based on the crystal structure of the LRF-POZ domain (refs. 32, 33, and Figure 7B). The protein interface that mediates dimerization includes 37 residues from each monomer (33). Among these 37 interface residues, 4 (I11, I20, L21, and Q27) were predicted to be key components (Figure 7B). To determine whether these residues are required for LRF dimer formation, we generated mammalian expression plasmids that encoded mutant LRF proteins harboring alanine substitutions at the respective loci (I11A, I20A, L21A, or Q27A). We coexpressed Flag-tagged and Xpress-tagged mutant LRF proteins in HEK293 cells and performed coimmunoprecipitation (Co-IP) (Figure 7C). Although all mutants weakly bound the WT protein (not shown), not all formed dimers. Alanine replacement of any of the 4 residues completely abrogated LRF dimerization (Figure 7D), indicating that each residue was essential for dimerization. These findings were confirmed by protein-fragment complementation assays (PCA) (34) in which the 5′ (hGLuc1) and 3′ (hGLuc2) sequences of the gene encoding the humanized form of *Gaussia princeps* luciferase (hGLuc) were fused to human LRF-POZ–coding sequences with nuclear localization sequences and the resulting fusions (LRF-POZ-hGLuc1 and LRF-POZ-hGLuc2) were coexpressed in HEK293 cells (Figure 7E). GCN4 leucine zipper protein served as a positive control (Zip-hGLuc1 and Zip-hGLuc2) (34). LRF-POZ induced complementation of hGLuc fragments, reconstituting hGLuc activity in a dose-dependent manner (Figure 7F). This reaction was LRF-POZ specific, as the combination of 2 unbound proteins (Zip-hGLuc1 and LRF-POZ-hGLuc2) failed to reconstitute hGLuc activity (Figure 7F). Next we tested the hGLuc reconstitution capacity of each of the mutant LRF-POZ proteins incapable of dimerization (Figure 7G). Although WT LRF-POZ displayed high luciferase activity, the I20A mutant did not, suggesting that it did not form dimers in cells. Both WT and mutant (I20A) protein were expressed at similar levels, as revealed by Western blot (Figure 7G). To further determine whether LRF-POZ proteins form dimers, we performed analytical ultracentrifugation (AUC) employing recombinant human LRF-POZ protein prepared in bacteria. The radial absorbance of the WT LRF-POZ and I20A mutant, collected at 4 speeds, was fit to a dimeric model. The calculated dimerization constant for the WT LRF-POZ was 0.65 μM, whereas the dimerization constant of I20A-LRF was 2.2 μM, or greater than 3-fold weaker (Figure 7H). In other words, at low expression levels, the majority of the I20A mutant will be monomeric, consistent with our findings in Co-IP and PCA experiments. Taken together, these data indicate that LRF forms a dimer in B cells and any of 4 interface residues (I11, I20, L21, and Q27) is required for dimer formation.

*Dimer formation is necessary for LRF function in B cells*. Although LRF forms an obligate dimer in cells, its significance for LRF function remains unknown. To address this question, we first tested to determine whether dimerization-deficient LRF mutants repressed p19Arf reporter activity. The I20A mutant, which cannot form dimers in cells (Figure 7), failed to repress the p19Arf reporter activity (Figure 8A). Lrf-deficient ($Lrf^{-/-}$) MEFs demonstrated senescence due to high p19Arf levels, and exogenous expression of Lrf could rescue this phenotype (11). To determine whether dimerization-deficient Lrf could rescue the senescence phenotype, WT or I20A-Lrf was retrovirally expressed in $Lrf^{-/-}$ MEFs and growth curves generated. WT-Lrf, but not I20A-Lrf, restored growth of $Lrf^{-/-}$ MEFs, indicating that LRF dimer formation is required for p19Arf repression in cells (Figure 8B).

Finally, to determine the functional significance of Lrf dimer formation in the context of GCB cell development, we examined whether dimerization-deficient Lrf could rescue the defective GC formation seen in $Lrf^{Flox/Flox}$ mb-1 $Cre^+$ mice. To express WT and I20A-Lrf specifically in B cells, a "B cell–specific" lentivirus vector, in which WT or I20A-Lrf expression was driven by the human CD19 promoter, was constructed (Figure 8C). BM HSCs were harvested from donor $Lrf^{Flox/Flox}$ mb-1 $Cre^+$ mice after 5-fluorouracil (5-FU) injection, transduced with empty lentivirus vector or vectors encoding either WT or I20A-Lrf, and transferred to lethally irradiated $CD45.1^+$ recipient mice. Recipient mice were immunized with

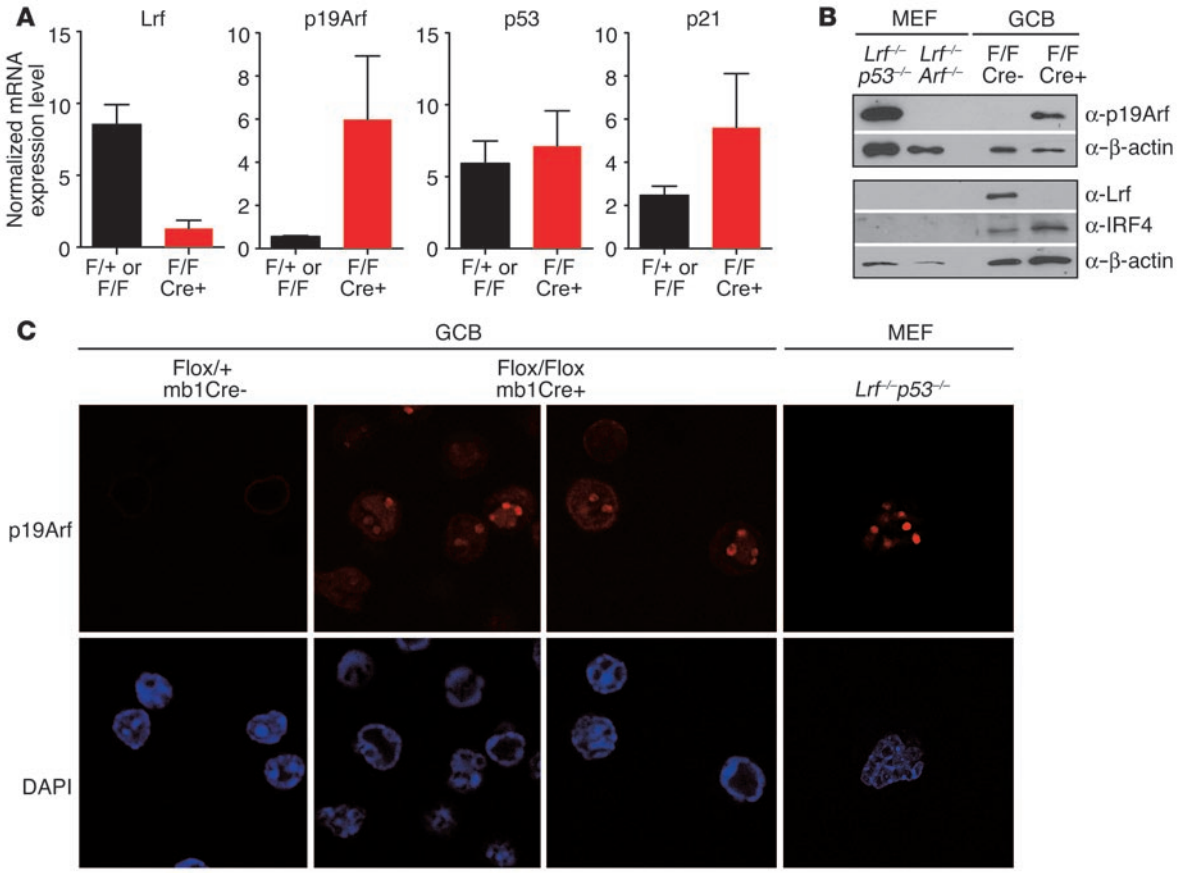


**Figure 5**
Loss of the *Lrf* gene leads to p19Arf upregulation in GCB cells. (**A**) GCB cells were FACS sorted and mRNA levels of Lrf, p19Arf, p53, and p21 measured by quantitative RT-PCR and normalized to corresponding *Hprt1* mRNA levels. Data represent mean with SD. (**B**) GCB cells were FACS sorted and Western blot for p19Arf, Lrf, Irf4, and β-actin performed. Protein extracts obtained from $Lrf^{-/-}p53^{-/-}$ and $Lrf^{-/-}p19Arf^{-/-}$ MEFs were used as positive and negative controls for p19Arf expression, respectively. Irf4 protein was only detected in GCB cell samples, confirming enrichment of GCB cells. Lrf protein was only detected in control GCB cells. (**C**) Immunofluorescence analysis of p19Arf protein in FACS-sorted GCB cells. p19ARF protein accumulated in nucleoli of Lrf-deficient GCB cells. $Lrf^{-/-}p53^{-/-}$ MEFs are shown as a positive control for p19Arf stain (red). Nuclei were counterstained with DAPI (blue). Original magnification, ×630.

SRBCs 2 months after transplantation and GC formation analyzed 1 week after immunization (Figure 8D). GFP expression was almost exclusively limited to B cells in recipient mice, confirming B cell–specific expression of the transgene (Figure 8E). Nontransduced ($GFP^-$) $CD45.2^+$ cells successfully gave rise to B cells in recipient spleen, but barely formed GCs in response to TD antigen, underscoring the cell-autonomous and B cell–intrinsic defects in GCB formation in the absence of the *Lrf* gene. More importantly, WT Lrf–expressing B cells could readily respond to TD antigen and differentiate into GCB cells, while neither empty vector–transduced nor I20A-Lrf–transduced B cells could develop GCB cells (Figure 8E). WT Lrf–transduced B cells gave rise to GCB cells 30–60 times more efficiently than empty vector– or I20A-Lrf–transduced cells (Figure 8F). Taken together, these in vivo rescue experiments strongly indicate that Lrf is essential for GCB formation in a B cell–intrinsic manner and dimer formation is critical for this function.

## Discussion

Elucidating the molecular features of normal B cell development is important, as this information could lead to the development of new target therapies for B cell malignancies and autoimmune diseases. In this study, we demonstrated critical roles for the Lrf protooncogene in normal B cell development and function, using B cell–specific Lrf-KO mouse models. We also showed that shRNA-mediated LRF knockdown was toxic to a subset of lymphoma cell lines, suggesting that LRF could be a therapeutic target for B cell malignancies. Since LRF dimer formation was a prerequisite for its function, the binding interface of the LRF dimer may be an attractive target for pharmacological blockage of LRF function.

Lrf is indispensable for B cell lineage commitment from HSCs/progenitors, as LRF-deficient HSCs/progenitors ($Lrf^{Flox/Flox}$ Mx-1 $Cre^+$) give rise to T cells in the BM at the expense of B cells (13). Lrf inactivation leads to activation of the Notch pathway via yet-unknown mechanisms, forcing HSCs/progenitors to differentiate toward the T cell lineage. Treatment with γ secretase inhibitor restores normal B cell development in the BM (13), suggesting Lrf is dispensable for the maintenance of BM B cells, despite its critical role in lineage fate determination. To specifically inactive the LRF gene in "committed" B cells, we employed mb-1 Cre mice, in which Cre expression was restricted to B cells after the pro–B cell stage (24). As expected, BM B cell compartments were grossly normal in $Lrf^{Flox/Flox}$ mb-1 $Cre^+$ mice (Supplemental

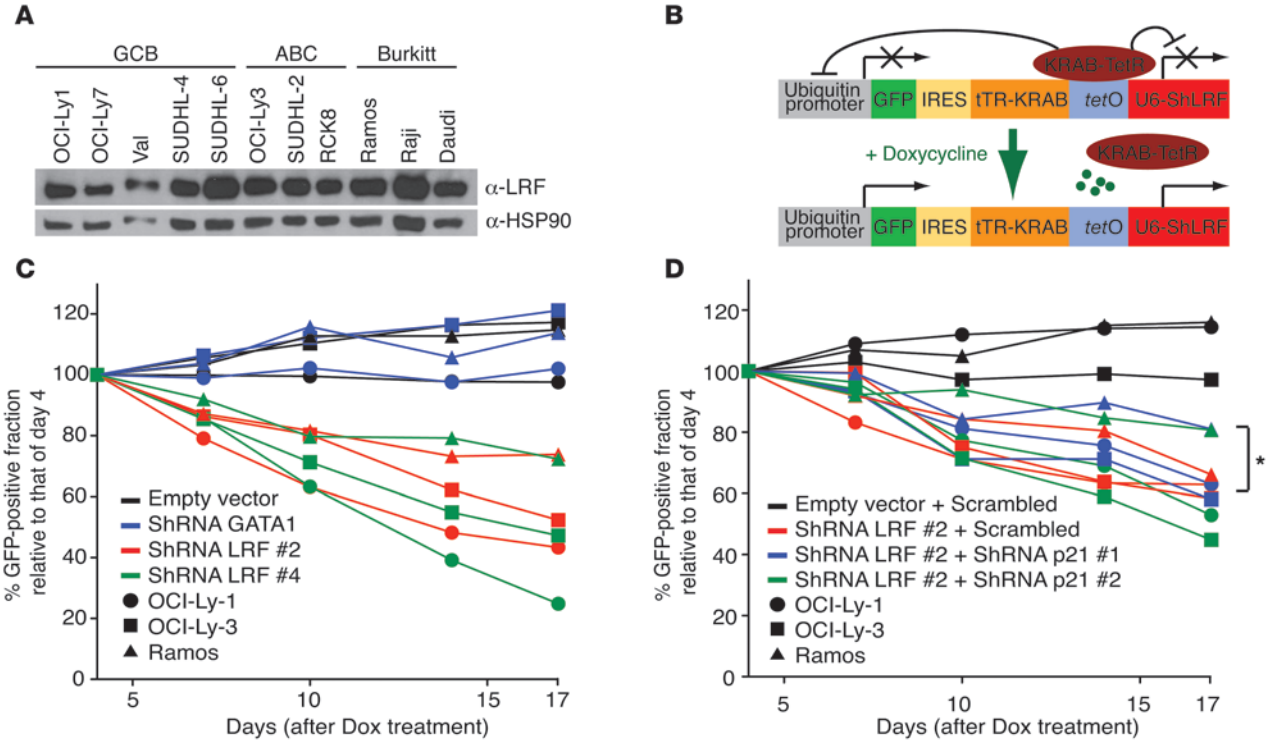


**Figure 6**

LRF inactivation is toxic to NHL cell lines. (**A**) Western blot analysis for LRF protein in 11 NHL lymphoma cell lines (5 GCB, 3 ABC, and 3 Burkitt-type lymphoma cell lines). (**B**) Schematic representation of a Dox-controllable single lentiviral vector system. (**C**) Lymphoma cell lines were transduced with a Dox-inducible lentivirus vector encoding an shRNA and GFP cassette, and the fraction of GFP-positive cells was measured at the indicated times by FACS. Proportion of GFP-positive fraction at each time point was normalized to that of day 4 after Dox treatment. Experiments were performed at least twice for each cell line, and representative results are shown. (**D**) shRNA toxicity assays were performed in the presence of shRNA-p21 as described in **C**. Cells expressing scrambled shRNAs were used as control. A proliferative advantage upon p21 knockdown was only observed in Ramos cells (asterisk).

Figure 1), indicating Lrf is not necessary for maintenance of B cells in the BM, once HSCs/progenitors commit to B cell lineage, as seen in Pu.1 KO mice (35).

We observed an increase in MZB cell numbers and concomitant decrease in FOB cell numbers in $Lrf^{Flox/Flox}$ mb-1 $Cre^{+}$ mice (Figure 1), which was reminiscent of the phenotype of Mint KO mice (5). Multiple signaling pathways, including Notch, BCR, and NF-κB, have been implicated in the regulation of MZB development (36). In particular, mutant mouse models lacking the components of Notch pathways (Notch2, ref. 2; RbpJκ, ref. 3; Dll1, ref. 1; Maml1, ref. 4; Mib1, ref. 21; Fringes, ref. 22; and Adam10, ref. 23) all demonstrated defects in MZB cell development and a concomitant increase in FOB cell numbers. Conversely, deletion of the *Mint/Sharp* gene, a suppressor of Notch signaling, led to an increase in MZB cells and reduction in FOB cells (5). These data clearly indicate that Notch2-mediated signals favor MZB fate at the branching point for the FOB versus MZB fate decision and regulate the balance between FOB and MZB development. Since Lrf interferes with Notch signals and maintains normal lymphoid lineage fate at the HSC/progenitor stages (13), we tested in vivo, using Lrf/Notch2 double-KO mice, whether LRF could also antagonize the Notch pathway in the context of mature B cells. Notch2 loss resulted in almost complete absence of MZB cells in Lrf-KO mice (Figure 1E) and, more importantly, total numbers of FOB cells were restored in $Lrf^{Flox/Flox}$ mb-1 $Cre^{+}$ mice (Figure 1F). Furthermore, Dll1 blockage almost completely rescued the excessive MZB cell differentiation to normal levels (Supplemental Figure 2D). These data do not provide direct evidence for epistasis between Lrf and Notch2. However, considering that Hes1, a Notch target gene, was upregulated in Lrf-deficient transitional B cells (Supplemental Figure 2A), we proposed a model in which LRF counteracts Notch2-mediated signals at the transitional B cell stages in a Notch ligand–dependent manner. It is worth noting that either Notch1 genetic loss, or Dll4, but not Dll1, blockage led to normal BM lymphoid development in $Lrf^{Flox/Flox}$ Mx-1 $Cre^{+}$ mice (S.U. Lee and T. Maeda, unpublished observations), reinforcing the idea that Lrf could target Notch pathways in a ligand-dependent and a cell context-specific manner.

LRF was originally identified as a promyelocytic leukemia zinc finger (also known as ZBTB16) homolog that interacts with the BCL6 oncoprotein (10). Lrf protein was coexpressed with Bcl6 in GCB cells (Supplemental Figure 6B). The *BCL6* gene is frequently mutated in NHL, and deregulated Bcl6 expression led to lymphoma development in mice (6, 9). Bcl6 is predominantly expressed in GCB cells and is indispensable for GC formation, presumably through both B cell–intrinsic and –extrinsic mechanisms (7, 8, 37). To determine the role of Lrf in GC formation and function, we immunized $Lrf^{Flox/Flox}$ mb-1 $Cre^{+}$ mice with TD antigens and examined their GC formation and immune response. GC formation was severely impaired in the absence of the *Lrf* gene, while a small

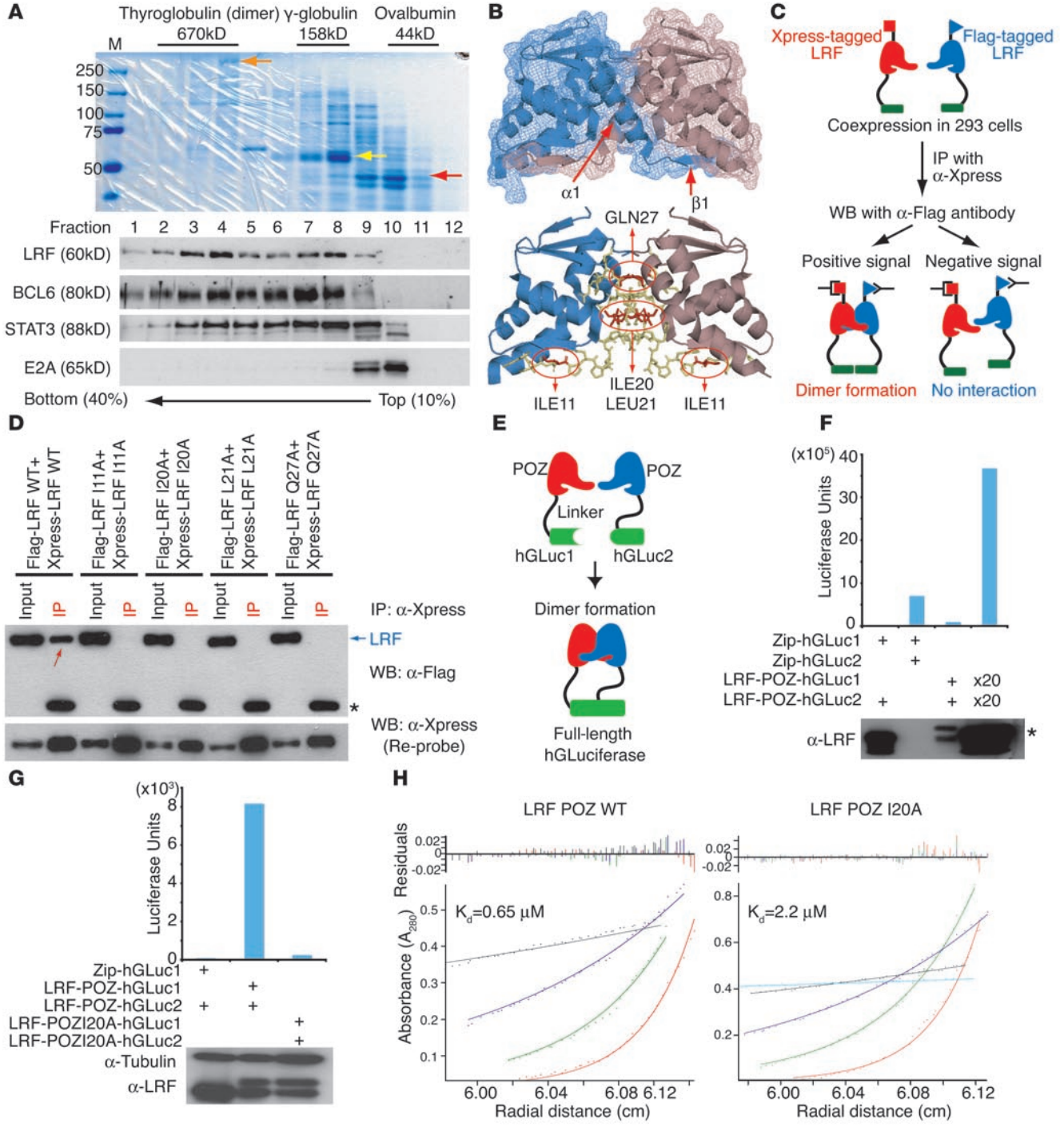


**Figure 7**

Identification of critical amino acid residues for LRF dimer formation. (**A**) Sucrose gradient analysis of LRF in Ly-1 nuclear extracts. The mobility of molecular mass standards was visualized by staining with Coomassie blue. Red, yellow, and orange arrows represent ovalbumin (44 kDa), bovine γ-globulin heavy chain (60 kDa), and thyroglobulin (335 kDa), respectively. Western blots were also performed using the protein samples from each fraction. (**B**) Proposed LRF dimer structure based on the 2NN2 PDB file. 4 critical residues within the interface are indicated. ILE, isoleucine; LEU, leucine; GLN, glycine. (**C**) Pairs of differentially tagged WT or LRF proteins mutated in 1 critical residue were coexpressed in 293 cells and immunoprecipitated with anti-Xpress. (**D**) Representative Co-IP experiment. Signals indicating dimerized Flag- and Xpress-tagged LRF proteins (red arrow) are seen only when both tagged proteins are WT. Asterisk indicates IgH chain of anti-Xpress antibody. (**E**) Schematic representation of protein-fragment complementation assay (PCA). (**F**) Plasmids harboring PCA fusions were cotransfected and luciferase assays performed. Expression levels of transfected LRF-POZ proteins were determined by Western blot. 2 bands are seen in the third and fourth lanes (asterisk) because the molecular weights of LRF-POZ-hGLuc1 and LRF-POZ-hGLuc2 differ. (**G**) Mutant LRF-POZ protein (I20A) did not reconstitute hGLuc activity. (**H**) The hydrodynamic properties of the WT and I20A POZ domain were analyzed by sedimentation equilibrium experiments using AUC. Radial scans were collected at 280 nm and 20°C at 4 speeds and dimerization constants ($K_d$) calculated.

number of Bcl6-positive and LRF-negative GCB cells were evident (Figure 2C). This is in contrast to the phenotype seen in Bcl6-KO mice, in which complete lack of GC was observed (7, 8). Reduction in GCB cell numbers was also seen in $Lrf^{Flox/Flox}$ Cγ1 $Cre^{+}$ mice, where Cre expression was restricted to GCB cells (Figure 3, F and G), underscoring the notion that initiation of GC formation was largely intact, but "maintenance" of GCB cells was perturbed in the absence of the *Lrf* gene. Furthermore, the defect in GC formation in $Lrf^{Flox/Flox}$ mb-1 $Cre^{+}$ mice was not due to the reduction in FOB cell numbers, which is presumably caused by Notch activation (Figure 1), because GC formation was also affected in Notch2/LRF double-KO mice, in which normal FOB numbers were restored (Figure 2D).

The classical model of GC reaction is that GCB cells in the DZ extensively proliferate while undergoing SHM, migrate to the LZ, and compete for antigen binding. Only B cells that harbor high-affinity BCR receive T cell help and survive, while cells with low-affinity BCR undergo apoptosis (6). Recent live-imaging studies suggested that cells in 2 compartments could move bidirectionally and the maturation process may not be strictly segregated between 2 compartments (38–40). GCB cells in the DZ express higher levels of Cxcr4 and are more active in the cell cycle (28). Proportions of $Cxcr4^{hi+}$ GCB cells were significantly reduced in $Lrf^{Flox/Flox}$ mb-1 $Cre^{+}$ mice compared with controls (Figure 4F), and Lrf-deficient GCB cells proliferated less, as revealed by microarray gene expression analysis (Figure 4, A and B) and EdU incorporation assays (Figure 4, C and D). Furthermore, Lrf-deficient GCB cells underwent apoptosis at a higher frequency than controls (Figure 4G), indicating that defects in both proliferation and survival of GCB cells account for the reduced GCB cell numbers in $Lrf^{Flox/Flox}$ mb-1 $Cre^{+}$ mice.

The reduction in GCB cell numbers led to hindered immune response to the TD antigen. Levels of serum class-switched Ig titers were significantly lower in $Lrf^{Flox/Flox}$ mb-1 $Cre^{+}$ mice than in control mice (Figure 3). However, it was unexpected that the frequency of SHM was comparable among mice of both genotypes upon NP-CGG immunization (Supplemental Figure 3, C and D), since SHM is closely linked to cell division (41). Several possible reasons can be proposed for this. First, GC formation was not completely abrogated in $Lrf^{Flox/Flox}$ mb-1 $Cre^{+}$ mice and the remaining Lrf-deficient GCB cells, which proliferate less (about < 50%; Figure 4D), could be sufficient to demonstrate the diverse mutations. Second, Aid function per se was likely to be intact in the absence of Lrf, as the capacity of Lrf-deficient B cells to undergo CSR was unaffected in vitro (Supplemental Figure 3A) and Aid mRNA levels in Lrf-deficient GCB cells were equivalent to those of controls (not shown).

Little is known about transcriptional programs that regulate GCB cell proliferation and survival (6). Other than BCL6, few transcription factors are known to function in GCB cells. Pou2AF1 (also known as OBF1 and OCAB) was originally identified as a transcriptional coactivator that is essential for antigen-driven immune responses, and mice lacking the *Pou2af1* gene failed to form GCs (42). Bach2 is a B cell–specific transcription factor that contains a BTB/POZ domain and a bZIP domain, and its inactivation in mice results in reduced FOB and GCB cell numbers, leading to impaired immune response to both TD and TID antigens (43). Spi-B (44), an Ets family transcription factor, Mef2c (45), a NFAT interacting transcription factor, and Irf8 (46), an Irf family transcription factor, have been also implicated in GC formation in response to TD antigen. Our study sheds a new light on the transcriptional program during GC formation and introduces LRF as a new transcription factor involved in regulating GCB cell proliferation and survival. However, questions remain as to how LRF activity is regulated during the GC response and how it collaborates with other transcription factors and transcriptional modifiers. In the context of terminal erythroid differentiation, the Gata factor directly binds the Lrf promoter and transcriptionally upregulates its expression (12). However, Lrf mRNA was abundantly expressed throughout mature B cell differentiation stages and reduced at the GC stage (Supplemental Figure 6A), when Lrf protein was highly expressed (Supplemental Figure 6, B and C). Therefore, Lrf protein levels are likely maintained at high levels through posttranscriptional mechanisms during the GC reaction. It is therefore possible that Lrf protein is stabilized and activated upon interaction with specialized T cells, such as FO helper T cells.

We propose that impaired GCB cell proliferation and increased apoptosis was due, at least in part, to derepression of the *p19Arf* gene. The p53 pathway plays a central role in control of the cell cycle and apoptosis in GCB cells while they proliferate and undergo genomic modifications, such as SHM and CSR. BCL6 prevents GCB cells from cell-cycle arrest and apoptosis caused by genotoxic stress (e.g., extensive cell division, SHM, and CSR) through p53-dependent and -independent mechanisms (47). BCL6 may also regulate GCB cell survival by transcriptionally repressing ATR (ataxia telangiectasia and Rad3 related), a critical sensor of DNA damage (48). Our data suggest that Lrf maintains p19Arf expression at low levels via direct transcriptional repression, allowing GCB cells to exponentially proliferate during the GC response. Although p19Arf is not thought to be directly activated in response to DNA damage (49), Lrf could also secure GCB cell proliferation and survival in the presence of genotoxic stress (e.g., CSR, SHM) by regulating the p53 pathway via p19Arf repression. Since Lrf and Bcl6 synergistically enhance MEF proliferation (11), it is tempting to speculate that Lrf and Bcl6 act together during GCB formation to maintain GCB cell proliferation and survival.

LRF was highly expressed in human DLBCL tissues (11) and B cell lymphoma cell lines (Figure 6A). In addition, Lrf overexpression in MEFs results in oncogenic transformation, while loss of the *Lrf* genes leads to cellular senescence due to derepression of the *p19Arf* gene (11). Moreover, overexpression of Lrf in immature B and T cells in mice leads to development of fatal lymphoblastic leukemia/lymphoma (11). Although these data clearly indicate that LRF could act as a protooncogene, it was unclear whether inactivation of the *Lrf* gene in cancerous cells could affect their proliferation and/or survival. Given that Lrf was necessary for GCB cell maintenance in mice, we examined the effect of LRF inactivation in NHL lymphoma cells, which presumably originated from GCB cells. LRF knockdown was toxic to a subset of B cell lymphoma cell lines (Figure 6C). Considering most lymphoma cell lines harbor the p53 mutation (50), it is likely that LRF could also exert its activity through p53-independent mechanisms. In fact, proliferation of shRNA-LRF–expressing cells was not restored in a subset of lymphoma cells upon knockdown of p21, a p53 target gene (Figure 6D). Thus, ARF/p53-independent LRF function, such as repression of the proapoptotic factor BIM (also known as BCL2L11) (12), and/or p53-independent ARF function (49) might account for the toxic effects of LRF shRNA. In fact, *BIM* mRNA was upregulated in LRF-shRNA–expressing ($GFP^{+}$) Ly-1 cells compared with $GFP^{-}$ cells (Supplemental Figure 5F).

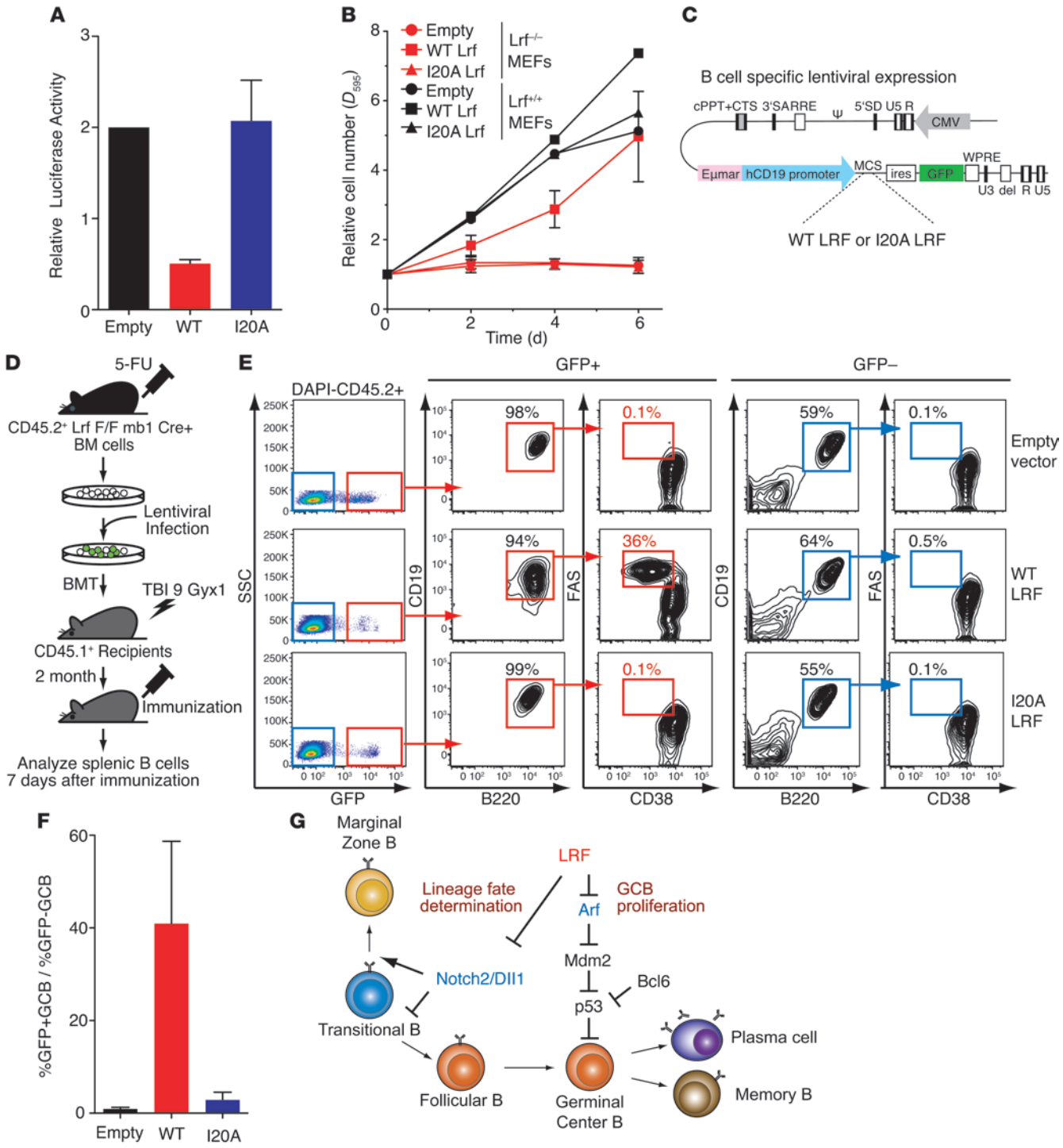


**Figure 8**

Dimer formation is required for LRF function in B cells. (**A**) Transrepression assays in *Lrf*$^{-/-}$*p19Arf*$^{-/-}$ immortalized MEFs transfected with empty vector, WT Lrf, or dimerization-deficient (I20A) Lrf expression vector along with mouse p19Arf luciferase-based reporter. Data represent mean with SD. (**B**) Growth curves of *Lrf*$^{+/+}$ and *Lrf*$^{-/-}$ MEFs after infection with empty, WT, or I20A Lrf retroviral vector. *y* axis shows relative cell numbers measured by attenuance (**D**) at 595 nm. Error bars indicate SD. (**C**) Schematic representation of the CSEμmarCD19-IRES-GFP vector. (**D**) BM HSCs were harvested from CD45.2$^{+}$ Lrf$^{Flox/Flox}$ mb-1 Cre$^{+}$ mice after 5-FU injection, infected with B cell–specific lentivirus, and transferred to CD45.1$^{+}$ recipient mice. The recipient mice were immunized 2 months after transplantation and GC formation analyzed 7 days after immunization. (**E**) Representative FACS profiles of GCB cell development in recipient mice. GFP was predominantly expressed in B cells (B220$^{+}$CD19$^{+}$), confirming B cell–specific transgene expression. Only WT-Lrf–transduced CD45.2$^{+}$ donor B cells (from Lrf$^{Flox/Flox}$ mb-1 Cre$^{+}$ mice) could give rise to GCB cells upon immunization. (**F**) Bar graph showing ratios between GFP-negative and -positive GCB cells within total CD45.2$^{+}$ GCB cells for each group (4 mice per group). Error bars indicate SD. (**G**) Key roles of LRF in mature B cell lineage fate and GC reaction. LRF may regulate FOB versus MZB lineage fate determination by counteracting the Notch2/Dll1 pathway, while it regulates GCB cell proliferation and survival by repressing *ARF*.

To obtain more mechanistic insights as to how LRF functions in B cells, we determined the amino acid residues necessary for LRF dimer formation and explored their functional significance in vitro and in vivo. Dimerization of LRF was critical for LRF function, as dimer-deficient Lrf did not repress p19Arf transcription (Figure 8A) or rescue the *Lrf*$^{-/-}$ MEF senescence phenotype (Figure 8B). More importantly, dimer-deficient Lrf was not functional in the context of GC formation, as it failed to rescue the GC phenotype seen in Lrf$^{Flox/Flox}$ mb-1 Cre$^{+}$ mice, while WT Lrf-expressing B cells readily formed GCs in vivo (Figure 8E). These data strongly indicate that LRF forms a dimer in B cells and that dimer formation is a prerequisite to its function. Furthermore, they suggest that interfering with dimer formation via small molecules or peptides could lead to inactivated LRF function.

Taken together, our studies have identified a new factor involved in regulating mature B cell lineage fate and GCB cell maintenance via distinct mechanisms (Figure 8G). They also provide further rationale for targeting LRF for the treatment of B cell malignancies, as LRF inactivation in transformed B cells attenuated their growth rate.

## Methods

*Mice*. Lrf and Notch2 conditional mutant mice were described previously (2, 13). The mb-1 Cre mice were provided by Michael Reth (Max-Planck Institute of Immunobiology and Epigenetics, Freiburg, Germany). B cell-specific Lrf conditional KO mice were obtained by crossing Lrf$^{Flox/Flox}$ mice with the mb-1 Cre or Cγ1 Cre$^{+}$ knockin mutant strain (24, 25). All mice were housed at the City of Hope (COH) Animal Resources Center in HEPA-filtered microisolation barrier-type cages with sterilized bedding and received autoclaved water. All animal experiments were approved by the Institutional Animal Care and Use Committee of the Beckman Research Institute of City of Hope, according to national, state, and institutional guidelines.

*Microarray analysis*. Lrf KO (Lrf$^{Flox/Flox}$ mb-1 Cre$^{+}$) and control (Lrf$^{Flox/+}$ mb-1 Cre$^{+}$) mice (4 each) were immunized with SRBC, and GCB cells were FACS sorted 7 days later. RNA samples were prepared using the Absolutely RNA Microprep Kit (Stratagene). Synthesis and labeling of cDNA targets and hybridization and scanning of GeneChips were carried out by the Microarray Core Facility at COH. Due to limited starting material, we used a modified 2-cycle amplification protocol. Briefly, cRNA was generated using 10 ng total RNA, according to the manufacturer's protocol, by using Affymetrix's GeneChip Whole Transcript Sense Target Labelling Assay in the first cycle of amplification. The cRNA was subjected to the RiboMinus Kit (Invitrogen) to remove rRNA. The resulting cRNA was used as the template for another round of amplification using the sense target labeling assay kit. Hybridization cocktails containing 5.5 μg of fragmented, end-labeled cDNA were prepared and applied to GeneChip Mouse Gene 1.0 ST arrays (GPL6246; Affymetrix). Hybridization was performed for 16 hours, and the arrays were washed and stained with the GeneChip Fluidics Station 450 using FS450_0007 script. Arrays were scanned at 5 μm resolution using the Affymetrix GCS 3000 7G and GeneChip Operating Software v. 1.4 to generate CEL intensity files. The raw data were normalized by Robust Multi-Array Average (RMA) using Affymetrix Expression Console (Agilent Technologies). Genes whose normalized data values were greater or less by more than 1.5-fold between 2 groups were selected and functional annotation performed using DAVID tools (http://david.abcc.ncifcrf.gov/) (26). Microarray data have been deposited in GEO (accession number GSE28449).

*Statistics*. *P* values were determined by 2-tailed Mann-Whitney *U* test using Prism software (GraphPad software), unless otherwise indicated. Two-tailed unpaired *t* test was used to determine significance of changes in GCB apoptosis rates (Figure 4G) and relative mRNA levels (Figure 5A). $P < 0.05$ was considered significant.

## Acknowledgments

We thank Michael Reth for providing the mb-1 Cre mice. We thank Donna Isbell, Jeremy LaDou, Michele Cuevas, and other COH Animal Resources members for maintenance of mouse colonies; David DiGiusto, Lucy Brown, and other Analytical Cytometry Core facility members for assistance with FACS sorting; Yate-Ching Yuan, Zheng Liu, and other Biomedical Informatics Core members for help with microarray experiments; Rumana Rashid for assistance and advice for protein purification; Claudia Kowolik for help with the shRNA study; Brian Armstrong for assistance with confocal microscopy experiments; Silvia R. da Costa and Keely Walker for critical reading of the manuscript; and Pier Paolo Pandolfi, Davide Robbiani, Ka Ming Pang, Stephen J. Forman, Vu Ngo, Christine Chuong, Bonnie Notthoff, and other members in the Division of HSC and Leukemia Research for assistance, advice, and helpful discussion. This work is supported in part by grants to T. Maeda from STOP Cancer, the V Foundation, the Margaret E. Early Medical Research Trust, the Tim Nesvig Lymphoma Research Fund, the American Society of Hematology, and the NIH (1R01AI084905-01A1).

Received for publication November 5, 2010, and accepted in revised form April 13, 2011.

Address correspondence to: Takahiro Maeda, Division of Hematopoietic Stem Cell and Leukemia Research, Beckman Research Institute of City of Hope, 1500 E. Duarte Rd., Duarte, California 91010, USA. Phone: 626.359.8111, ext. 68824; Fax: 626.301.8973; E-mail: tmaeda@coh.org.

1. Hozumi K, et al. Delta-like 1 is necessary for the generation of marginal zone B cells but not T cells in vivo. *Nat Immunol*. 2004;5(6):638–644.
2. Saito T, et al. Notch2 is preferentially expressed in mature B cells and indispensable for marginal zone B lineage development. *Immunity*. 2003; 18(5):675–685.
3. Tanigaki K, et al. Notch-RBP-J signaling is involved in cell fate determination of marginal zone B cells. *Nat Immunol*. 2002;3(5):443–450.
4. Wu L, Maillard I, Nakamura M, Pear WS, Griffin JD. The transcriptional coactivator Maml1 is required for Notch2-mediated marginal zone B-cell development. *Blood*. 2007;110(10):3618–3623.
5. Yabe D, et al. Generation of a conditional knockout allele for mammalian Spen protein Mint/SHARP. *Genesis*. 2007;45(5):300–306.
6. Klein U, Dalla-Favera R. Germinal centres: role in B-cell physiology and malignancy. *Nat Rev Immunol*. 2008;8(1):22–33.
7. Dent AL, Shaffer AL, Yu X, Allman D, Staudt LM. Control of inflammation, cytokine expression, and germinal center formation by BCL-6. *Science*. 1997;276(5312):589–592.
8. Ye BH, et al. The BCL-6 proto-oncogene controls germinal-centre formation and Th2-type inflammation. *Nat Genet*. 1997;16(2):161–170.
9. Cattoretti G, et al. Deregulated BCL6 expression recapitulates the pathogenesis of human diffuse large B cell lymphomas in mice. *Cancer Cell*. 2005;7(5):445–455.
10. Davies JM, et al. Novel BTB/POZ domain zinc-finger protein, LRF, is a potential target of the LAZ-3/BCL-6 oncogene. *Oncogene*. 1999;18(2):365–375.
11. Maeda T, et al. Role of the proto-oncogene Pokemon in cellular transformation and ARF repression. *Nature*. 2005;433(7023):278–285.
12. Maeda T, et al. LRF Is an Essential Downstream Target of GATA1 in Erythroid Development and Regulates BIM-Dependent Apoptosis. *Dev Cell*. 2009; 17(4):527–540.
13. Maeda T, et al. Regulation of B versus T lymphoid lineage fate decision by the proto-oncogene LRF. *Science*. 2007;316(5826):860–866.
14. Kumano K, et al. Notch1 but not Notch2 is essential for generating hematopoietic stem cells from endothelial cells. *Immunity*. 2003;18(5):699–711.
15. Kopan R, Ilagan MX. The canonical Notch signaling pathway: unfolding the activation mechanism. *Cell*. 2009;137(2):216–233.
16. Radtke F, et al. Deficient T cell fate specification in mice with an induced inactivation of Notch1. *Immunity*. 1999;10(5):547–558.
17. Han H, et al. Inducible gene knockout of transcrip-

tion factor recombination signal binding protein-J reveals its essential role in T versus B lineage decision. *Int Immunol*. 2002;14(6):637–645.
18. Hozumi K, et al. Delta-like 4 is indispensable in thymic environment specific for T cell development. *J Exp Med*. 2008;205(11):2507–2513.
19. Pui JC, et al. Notch1 expression in early lymphopoiesis influences B versus T lineage determination. *Immunity*. 1999;11(3):299–308.
20. Weng AP, et al. Activating mutations of NOTCH1 in human T cell acute lymphoblastic leukemia. *Science*. 2004;306(5694):269–271.
21. Song R, et al. Mind bomb 1 in the lymphopoietic niches is essential for T and marginal zone B cell development. *J Exp Med*. 2008;205(11):2525–2536.
22. Tan JB, et al. Lunatic and manic fringe cooperatively enhance marginal zone B cell precursor competition for delta-like 1 in splenic endothelial niches. *Immunity*. 2009;30(2):254–263.
23. Gibb DR, et al. ADAM10 is essential for Notch2-dependent marginal zone B cell development and CD23 cleavage in vivo. *J Exp Med*. 2010; 207(3):623–635.
24. Hobeika E, et al. Testing gene function early in the B cell lineage in mb1-cre mice. *Proc Natl Acad Sci U S A*. 2006;103(37):13789–13794.
25. Casola S, et al. Tracking germinal center B cells expressing germ-line immunoglobulin gamma1 transcripts by conditional gene targeting. *Proc Natl Acad Sci U S A*. 2006;103(19):7396–7401.
26. Huang da W, Sherman BT, Lempicki RA. Systematic and integrative analysis of large gene lists using DAVID bioinformatics resources. *Nat Protoc*. 2009;4(1):44–57.
27. McHeyzer-Williams MG, McLean MJ, Lalor PA, Nossal GJ. Antigen-driven B cell differentiation in vivo. *J Exp Med*. 1993;178(1):295–307.
28. Allen CD, et al. Germinal center dark and light zone organization is mediated by CXCR4 and CXCR5. *Nat Immunol*. 2004;5(9):943–952.
29. Szulc J, Wiznerowicz M, Sauvain MO, Trono D, Aebischer P. A versatile tool for conditional gene expression and knockdown. *Nat Methods*. 2006; 3(2):109–116.
30. Melnick A, et al. In-depth mutational analysis of the promyelocytic leukemia zinc finger BTB/POZ domain reveals motifs and residues required for biological and transcriptional functions. *Mol Cell Biol*. 2000;20(17):6550–6567.
31. Stogios PJ, Downs GS, Jauhal JJ, Nandra SK, Privé GG. Sequence and structural analysis of BTB domain proteins. *Genome Biol*. 2005;6(10):R82.
32. Schubot FD, Tropea JE, Waugh DS. Structure of the POZ domain of human LRF, a master regulator of oncogenesis. *Biochem Biophys Res Commun*. 2006; 351(1):1–6.
33. Stogios PJ, Chen L, Prive GG. Crystal structure of the BTB domain from the LRF/ZBTB7 transcriptional regulator. *Protein Sci*. 2007;16(2):336–342.
34. Remy I, Michnick SW. A highly sensitive protein-protein interaction assay based on Gaussia luciferase. *Nat Methods*. 2006;3(12):977–979.
35. Iwasaki H, et al. Distinctive and indispensable roles of PU.1 in maintenance of hematopoietic stem cells and their differentiation. *Blood*. 2005;106(5):1590–1600.
36. Pillai S, Cariappa A. The follicular versus marginal zone B lymphocyte cell fate decision. *Nat Rev Immunol*. 2009;9(11):767–777.
37. Nurieva RI, et al. Bcl6 mediates the development of T follicular helper cells. *Science*. 2009; 325(5943):1001–1005.
38. Allen CD, Okada T, Tang HL, Cyster JG. Imaging of germinal center selection events during affinity maturation. *Science*. 2007;315(5811):528–531.
39. Schwickert TA, et al. In vivo imaging of germinal centres reveals a dynamic open structure. *Nature*. 2007;446(7131):83–87.
40. Hauser AE, et al. Definition of germinal-center B cell migration in vivo reveals predominant intrazonal circulation patterns. *Immunity*. 2007; 26(5):655–667.
41. French DL, Laskov R, Scharff MD. The role of somatic hypermutation in the generation of antibody diversity. *Science*. 1989;244(4909):1152–1157.
42. Schubart DB, Rolink A, Kosco-Vilbois MH, Botteri F, Matthias P. B-cell-specific coactivator OBF-1/OCA-B/Bob1 required for immune response and germinal centre formation. *Nature*. 1996;383(6595):538–542.
43. Muto A, et al. The transcriptional programme of antibody class switching involves the repressor Bach2. *Nature*. 2004;429(6991):566-571.
44. Su GH, et al. Defective B cell receptor-mediated responses in mice lacking the Ets protein, Spi-B. *EMBO J*. 1997;16(23):7118–7129.
45. Wilker PR, et al. Transcription factor Mef2c is required for B cell proliferation and survival after antigen receptor stimulation. *Nat Immunol*. 2008; 9(6):603–612.
46. Lee CH, et al. Regulation of the germinal center gene program by interferon (IFN) regulatory factor 8/IFN consensus sequence-binding protein. *J Exp Med*. 2006;203(1):63–72.
47. Phan RT, Dalla-Favera R. The BCL6 proto-oncogene suppresses p53 expression in germinal-centre B cells. *Nature*. 2004;432(7017):635–639.
48. Ranuncolo SM, et al. Bcl-6 mediates the germinal center B cell phenotype and lymphomagenesis through transcriptional repression of the DNA-damage sensor ATR. *Nat Immunol*. 2007;8(7):705–714.
49. Sherr CJ. Divorcing ARF and p53: an unsettled case. *Nat Rev Cancer*. 2006;6(9):663–673.
50. Drexler HG. *Guide to Leukemia-Lymphoma Cell Lines*. Braunschweig, Germany: Braunschweig; 2005.